JOURNAL OF GEOPHYSICAL RESEARCH, VOL. 99, NO. D6, PAGES 13,059–13,082, JUNE 20, 1994

Observations of lightning phenomena using radio interferometry

C. T. Rhodes,[1] X. M. Shao, P. R. Krehbiel, R. J. Thomas, and C. O. Hayenga[2]

Geophysical Research Center, New Mexico Institute of Mining and Technology, Socorro

Abstract.
A radio interferometer system is described which utilizes multiple baselines to determine the direction of lightning radiation sources with an angular resolution of a few degrees and with microsecond time resolution. An interactive graphics analysis procedure is used to remove fringe ambiguities from the data and to reveal the structure and development of lightning discharges inside the storm. Radiation source directions and electric field waveforms have been analyzed for different types of breakdown events for two lightning flashes. These include the initial breakdown and K type events of in-cloud activity, the leaders of initial and subsequent strokes to ground, and activity during and following return strokes. Radiation during the initial breakdown of one flash was found to consist of intermittent, localized bursts of radiation that were slow moving. Source motion within a given burst was unresolved by the interferometer but was detected from burst to burst, with negative charge being transported in the direction of the breakdown progression. Radiation during initial leaders to ground was similar but more intense and continuous and had a characteristic intensity waveform. Radiation from in-cloud K type events is essentially the same as for dart leaders; in both cases it is produced at the leading edge of a fast-moving negative streamer that propagates along a well-defined, often extensive, path. K type events are sometimes terminated by a fast field change that appears analogous to the field change of a return stroke. Dart leaders are sometimes observed to die out before reaching ground; these are termed "attempted leaders" and, except for their greater extent, are no different than K type events. Several modes of breakdown during and after return strokes have been documented and analyzed. One mode corresponds to the launching of a positive streamer away from the upper end of the leader channel, apparently as the return stroke reaches the leader start point. In another mode, the quenching of the dart leader radiation upon reaching ground reveals concurrent breakdown in the vicinity of the source region for the leader. In both instances the breakdown appears to establish channel extensions or branches that are followed by later activity of the flash. Finally, a new type of breakdown event has been identified whose electric field change and source development resemble those of an initial negative leader but which progresses horizontally through the storm. An example is shown which spawned a dart leader to ground.

Introduction

The most interesting parts of a lightning discharge occur inside the cloud where they are obscured from view at optical frequencies. Clouds are transparent at radio frequencies, however, and several techniques have been developed for locating RF radiation events inside the storm. Time-of-arrival techniques have been used to locate and study lightning radiation in two and three spatial dimensions [e.g., *Proctor*, 1976, 1981; *Taylor*, 1978; *Lennon*, 1975; *Proctor et al.*, 1988; *Rustan et al.*, 1980]. These techniques work best for locating isolated, impulsive radiation events but produce images of lightning which tend to be spatially noisy and difficult to interpret. Interferometric techniques allow the sources of nonimpulsive radiation events to be located and have continually improved as a means for study-

[1]Now at Los Alamos National Laboratories, Los Alamos, New Mexico.

[2]Now at Boulder, Colorado.

Paper number 94JD00318.
0148-0227/94/94JD-00318$05.00

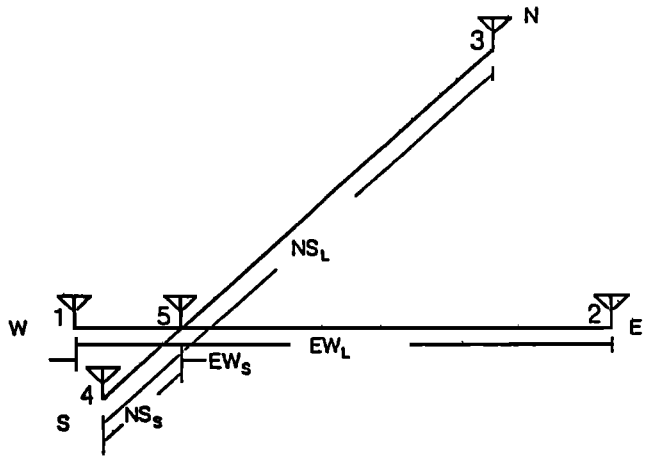

Figure 1. Configuration of the interferometer antennas. Five antennas were shared to produce short (0.5λ) and long (4λ) baselines in orthogonal directions.

ing discharge processes [*Hayenga*, 1979, 1984; *Warwick et al.*, 1979; *Hayenga and Warwick*, 1981; *Richard and Auffray*, 1985; *Richard et al.*, 1985, 1986; *Rhodes*, 1989; *Rhodes and Krehbiel*, 1989]. Much of the energy radiated by lightning at radio frequencies occurs in continuous bursts lasting several tens or hundreds of microseconds or longer, which is not amenable to location by time-of-arrival techniques. Interferometric techniques allow the radiation sources to be located as a function of time during the bursts and clearly delineate the breakdown channels.

A primary difficulty of using interferometry to study lightning is that multiple-wavelength baselines are needed to obtain the desired angular resolution, but such baselines have fringe ambiguities that need to be resolved. Short baseline measurements can be used to resolve the fringe amibiguities but have substantial systematic errors that adversely affect the fringe resolution. The systematic errors are caused by the interaction between the closely spaced antennas and also by the use of a finite ground plane for the antenna array. In addition, the phase measurements used to determine the source direction have random errors because of the stochastic nature of the radiation, which also adversely affect the ambiguity resolution. The combination of these effects complicates the analyses of interferometric observations.

In this paper we describe an interferometer developed at the New Mexico Institute of Mining and Technology for studying lightning radiation. We first discuss the interpretation of the measurements and then describe the approach used to analyze the observations. Then we present results from two lightning discharges which illustrate different types of discharge processes. The discharges which we discuss occurred over Socorro, New Mexico, during the summer of 1988.

The Interferometer System

The interferometer system used in this study measured the direction of arrival of VHF radiation with 1-μs time resolution and has been described in detail by *Rhodes* [1989]. Figure 1 shows the antenna array of the interferometer. Five antennas were configured to form long and short baselines along each of two orthogonal directions in a horizontal plane. Antennas were shared between baselines to reduce the number of receiving systems needed. The long baselines were 4λ in length and provided an accurate but ambiguous determination of the source direction. The short baselines were $\lambda/2$ in length and provided a coarse determination of the source direction for resolving the ambiguities of the long baseline measurements.

The interferometer operated at a center frequency of 274 MHz with a bandwidth of 6 MHz. The signal received by each antenna was prefiltered, amplified, and down-converted to 60 MHz intermediate frequency, then it was further amplified and transmitted by coaxial cable from the rooftop antenna installation to an interior room in our research building. Here the signals were limited in amplitude using constant-phase limiting amplifiers. Quadrature phase detectors were used to measure the phase difference ϕ of the signals from each baseline or pair of antennas. The outputs of the phase detectors were proportional to $I = A\cos\phi$ and $Q = A\sin\phi$, corresponding to the Cartesian components of a radial vector or phasor making an angle ϕ with respect to the I or x axis. This will be referred to as the "I-Q" vector, which was displayed during operation of the interferometer for monitor purposes. The amplitude limiting enabled the instrument to operate over a large dynamic range of input signal strength (70 dB) and made the I-Q vector have constant length for input signals larger than 3-6 dB above minimum detectable signal.

The I and Q signals were averaged with 1-μs running averagers to improve the accuracy of the phase estimate and were digitized at 1-μs time intervals for subsequent processing. Flash analog-to-digital converters with 7-bit resolution and 10 MHz digitizing capability were used. The resulting digital I and Q values were used as addresses to a read-only memory which performed an inverse tangent lookup operation to determine the phase difference $\phi = \tan^{-1}(Q/I)$. Four phase values were thus obtained, corresponding to the short and long baselines along the orthogonal directions. Each phase value consisted of an 8-bit digital word (2 quadrant bits and 6 additional bits), in which 0 to 2π phase difference was represented as 00-FF hexadecimal.

A separate antenna and receiver measured the amplitude of the RF radiation signal using a logarithmic detector, and a flat plate antenna was used to sense the electrostatic field change ΔE of the lightning discharge. The electric field change was sensed in the manner described by *Krehbiel et al.* [1979] using a decay time constant of 10 s; its signal was also differentiated with a decay time of 0.1 ms and amplified by a factor of 100 to give the fast components of ΔE. The RF amplitude and fast ΔE data values were digitized with 8-bit resolution in synchronization with the phase values and were combined with the phase values to form two 3-byte

data words per microsecond. These were recorded on a high-density digital magnetic tape recorder capable of continuous recording for 15 min between tape changes. A 1-bit serial housekeeping stream was also recorded, which contained time and the 10-s decay constant ΔE signal. The latter was digitized with 12-bit resolution at 20-μs time intervals and provided the electrostatic field change of the discharge. Flashes of interest were played back at a reduced rate into a computer for analysis.

Interpretation and Analysis of the Phase Measurements

For plane-wave radiation arriving at an angle θ with respect to an antenna baseline, the phase difference of the signal at the output of the long and short baselines is readily shown to be given by

$$\phi = \frac{2\pi}{\lambda} d \cos\theta = \begin{cases} \pi\cos\theta & d = \lambda/2 \\ 8(\pi\cos\theta) & d = 4\lambda = 8(\lambda/2), \end{cases} \quad (1)$$

where d is the antenna separation or baseline length and λ is the wavelength of the received radiation. The measured phase differences thus give the angle cosine, $\cos\theta$, of the source direction. For a $\lambda/2$ baseline , $\phi = \phi_{\text{short}}$ varies from $+\pi$ to $-\pi$ as the source direction varies from $\theta = 0$ to π. This corresponds to one complete rotation of the I-Q vector and provides an unambiguous indication of the source direction. For the 4λ or long baseline, $\phi_{\text{long}} = 8\phi_{\text{short}}$ and varies through eight sets of 2π, or eight "fringes", as the source direction varies from $\theta = 0$ to π. The term fringe refers to incoherent interferometric systems and implies the existence of maxima and minima (nulls) in the response pattern of a multiple aperture system. Such nulls do not exist in a coherent, quadrature system, but the terminology remains useful for describing the interferometer operation.

As the source direction θ varies, the I-Q vectors rotate in angle, with the long baseline vector rotating 8 times faster than the corresponding short baseline vector. The short and long baseline phases are therefore analogous to the hour and minute "hands" of a clock. This provides a useful analogy for understanding the interferometer operation: the short and long baselines in each direction indicate the source phase or direction in the same manner as the hour and minute hands of an 8-hour clock. In principle, the time (phase) of the clock can be determined from the hour hand ($\lambda/2$ baseline) alone, but the minute hand (long baseline) provides a vernier for more accurate determination. However, the minute hand alone does not provide information about the hour (fringe).

To show how the phase values are related to the source direction, it is useful to define a normalized phase $\phi' = \phi/\pi$, where ϕ is the accurate (short baseline) phase value that results from combining the short and long baseline phases. Defining the x axis of the coordinate system to lie along one of the baseline directions, we have from spherical trigonometry that

$$\phi'_x = \cos\alpha = \sin(Az)\cos(El) \quad (2)$$

and, for the orthogonal (y axis) baseline,

$$\phi'_y = \cos\beta = \cos(Az)\cos(El). \quad (3)$$

Here, α and β are the spherical angles of arrival with respect to each baseline direction (equivalent to θ in equation (1)) and Az and El are the azimuth and elevation of the source direction, respectively. The right-hand sides of (2) and (3) describe the projection of a point located at angles Az, El on a unit radius sphere onto the horizontal plane. The normalized phase values therefore correspond to such a projection.

The above result is illustrated graphically in Figure 2. The radiation sources in three-dimensional space are projected radially onto a "celestial" sphere of unit radius. The normalized phase values correspond to the projection of the celestial points onto the horizontal plane, that is, the plane of the antenna array. The azimuth and elevation angles are obtained from measured phase values by inverting equations (2) and (3), that is, by projecting the phase values upward onto the unit sphere. The circle in the phase or projection plane is termed the "unit circle" and corresponds to the horizon. The center of the phase plane/unit circle corresponds to the zenith.

Figure 2 illustrates a disadvantageous characteristic of using only horizontal baselines, namely, sources at low-elevation angles have their phase values compressed just inside the horizon circle. Errors in the phase measurements tend to have a constant value in the phase plane and therefore produce increasingly large elevation errors as the source elevation approaches the horizon. This effect can be important at angles as high as 30° above the horizon; sources below this elevation have their phase values compressed into an annular region between 0.77 and unity radius. Below 20° elevation the source phases are compressed between 0.94 and unity radius.

The above effect caused the interferometer of this study to function best for discharges that were at high elevation angles, that is, at close range. For more distant discharges, or at low altitude on the channel-to-ground of closer discharges, the interferometer functioned primarily as an azimuthal direction finder. If 10° is considered to be the lowest usefully determined elevation angle, the effective range of an interferometer for determining elevation is about 30 km for a source at 5 km altitude. The effect could be alleviated by tilting the plane of the antenna array in a preferred direction of observation or by incorporating a vertical baseline. The latter approach has been utilized by *Taylor* [1978] in a short baseline time-of-arrival system.

From Figure 2 it is clear that phase values outside the unit circle cannot correspond to physical sources. Receiver noise at each antenna, however, produces uncorrelated phase values that are uniformly distributed over the phase plane. This turns out to provide a useful test of the interferometer operation.

Combining the Short and Long Baseline Phases

Figure 3 shows an example of observational data in the phase or projection plane which illustrates the uncertainties of the observations and the problems involved in combining the short and long baseline phases. In this case the radiation was produced by an extensive dart leader that started southeast of the interferometer, passed nearly overhead, and went to ground to the north of the inteferometer. It progressed continuously along a well-defined path, requiring about about 1.5 ms to reach ground. As discussed above, the inscribed circle corresponds to the horizon, and the center of the phase plane corresponds to the zenith. The fringe ambiguities of the long baseline system are equally spaced in the phase plane and are denoted by the 8 x 8 square grid. The long baseline data provide an accurate measure of the source location within a small grid square, and the short baseline phases are used to estimate the actual square in which the sources originated.

Figure 3a shows the short baseline phases only, while Figure 3b shows the results of using the short baseline phases to estimate the long baseline fringe. As can be seen, the large scatter in the short baseline phases causes substantial aliasing in the combined phase estimates of Figure 3b, extending over several adjacent fringes. The aliasing is clearer when the combined phase values in each direction are plotted separately versus time, as in Figure 3c. For events whose source locations vary continuously and single-valuedly with time, such as in this example, it is a relatively simple matter to computationally displace the phase values over an integral number of fringes to make them continuous as in Figure 3d. The dealiased phases can then be plotted in the phase plane to reveal the true nature of the streamer (Figure 3e). The result can be displaced from

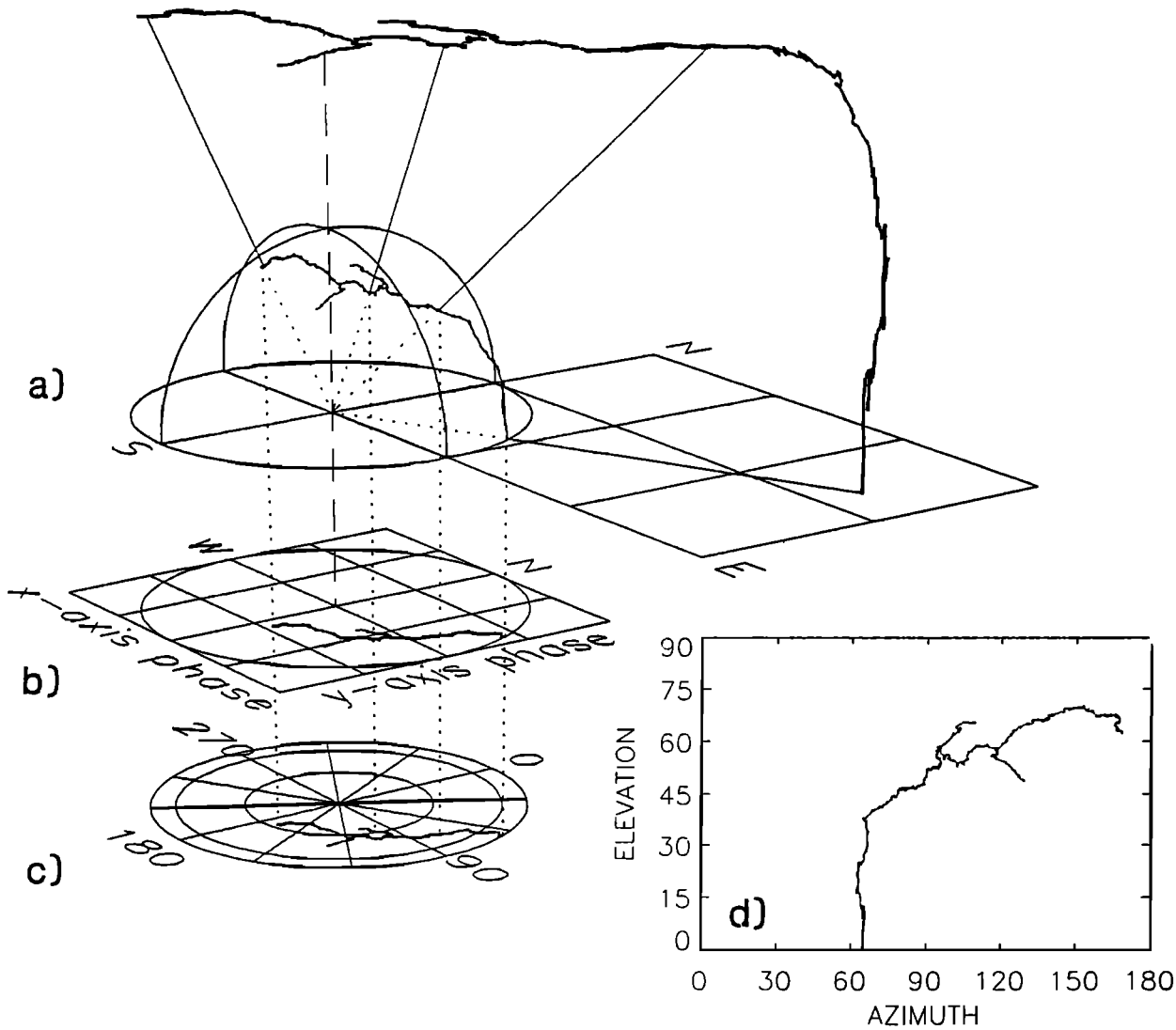

Figure 2. Interpretation of the interferometer measurements. (a) Radiation from the three-dimensional lightning channels can be considered as originating on a unit radius celestial hemisphere. (b) The normalized phase measurements from orthogonal baselines correspond to the projection of the sources from the celestial hemisphere onto the plane of the antenna array. (c),(d) In turn, the phase values indicate the azimuth and elevation of the sources.

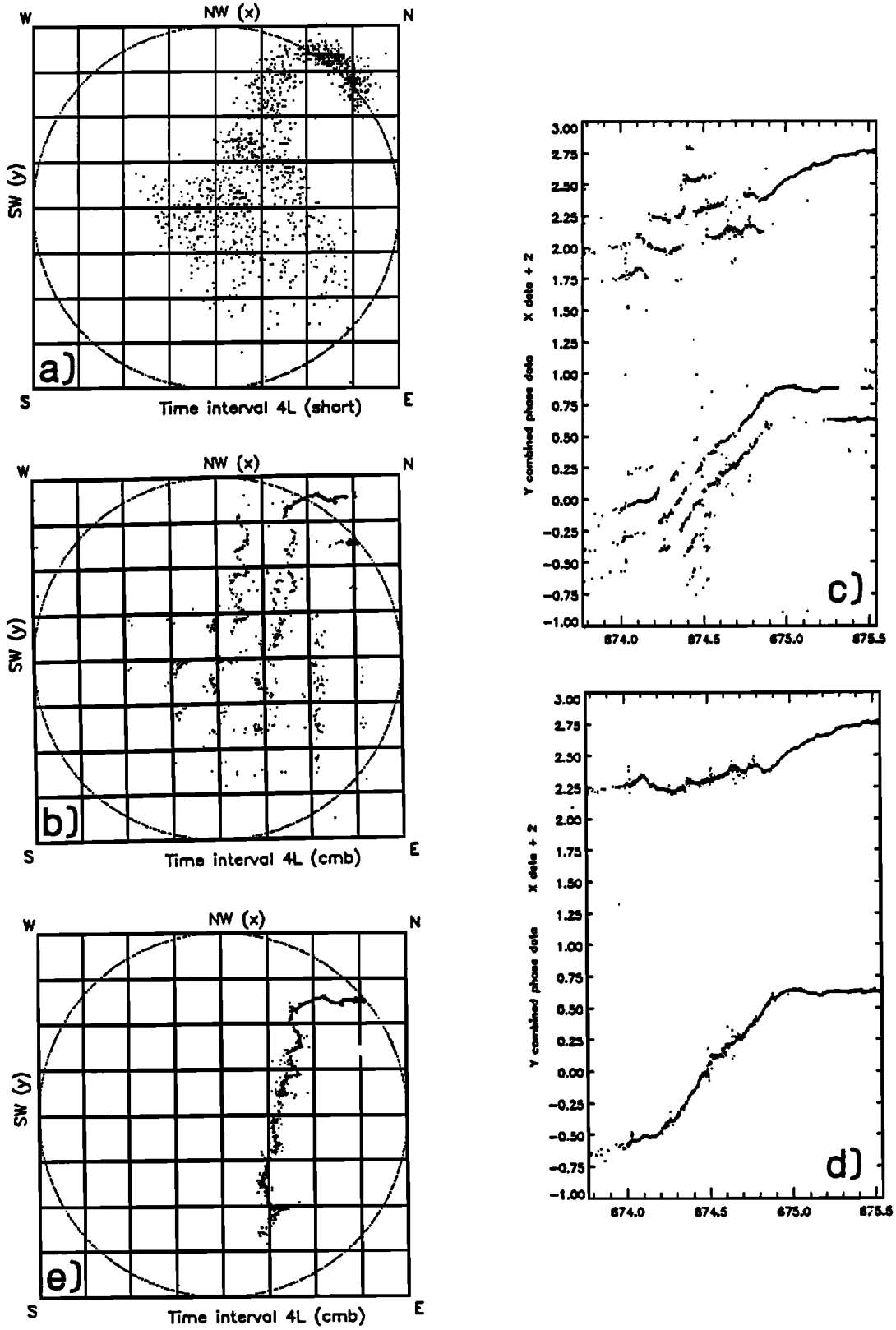

Figure 3. Phase data for a dart leader to ground, illustrating the phase combination process. (a) Short baseline phases only, showing the spread introduced by random and systematic errors. (b) Initial combination of short and long baseline phase values, showing aliasing and systematic errors. (c) Same as Figure 3b, except with the x and y phase values plotted versus time. (d) Same as Figure 3c, except with aliases and systematic errors removed by displacing phase values over an integral number of fringes. (e) Final result, in the phase or projection plane. (Leader is for stroke 4 of flash 153844 (Figure 11b).)

its correct location by an integral number of fringes if the phase values were shifted onto a wrong fringe in Figure 3c. In the case of dart leaders, the fact that the leader propagates to the horizon (the unit circle) usually enables the streamer to be placed in the correct location. Dart leaders thus provide an important framework for analyzing the remainder of a flash. Most radiation events are confined within a single fringe or progress through a couple of fringes, and are correctly located by comparison with known channels and the use of pattern recognition. When radiation is from a new channel segment, the fringe is identified from continuity considerations for the overall flash.

The above provides an interactive procedure for reconstructing a discharge from the phase observations. Although tedious and time-consuming, it has been used to produce self-consistent pictures of discharges that appear to be valid. The long baseline phases are implicitly assumed to be correct. (An improved antenna configuration, coupled with improved data processing techniques, has since significantly reduced the systematic errors and fringe ambiguity problem and enabled the processing to be done automatically and in real time [*Shao*, 1993].)

In contrast to the system of this study, *Hayenga and Warwick* [1981] utilized single, orthogonal baselines two wavelengths in extent, having a 4 x 4 fringe ambiguity grid, and resolved the fringe ambiguities from knowledge of the storm location and from physical considerations. *Richard et al.* [1986] utilized two equilateral triangular arrays: a small array having an antenna spacing of 1λ or 0.5λ and a large array of 10λ spacing. The latter would have a 20 x 20 fringe ambiguity grid in an orthogonal system; the use of nonorthogonal baselines somewhat reduces the number of ambiguities.

A simple algorithm helps to identify the long baseline fringe from the short baseline data and to reduce aliasing. In a given direction, the fringe number n is estimated to be the nearest integer n to $(8\phi'_{\text{short}} - \phi'_{\text{long}})$. The combined phase estimate is then

$$\hat{\phi}' = (n + \phi'_{\text{long}})/8 \,. \tag{4}$$

The algorithm corrects errors of up to one-half fringe in the short baseline data and is analogous to using the minute hand of a clock to correct errors of up to one-half hour in the position of the hour hand. The algorithm was used in the data of Figure 3c and significantly reduces the aliasing that would otherwise occur.

The scatter in the short baseline phases of Figure 3a is due to both random and systematic errors. Systematic error is seen as the leader neared ground, where the short baseline phase values lie in the physically impossible region outside the unit circle. (This was not due to a simple offset in phase, as a continuously pulsed calibration source was used to remove phase offsets.) The systematic error changed with source location or direction, as evidenced by "jumping" of the dominant fringe in the plots of Figures 3b and 3c.

The systematic errors result primarily from interaction between the closely spaced antennas and from the effects of a finite ground plane. The effect of antenna interaction has been discussed by *Richard and Auffray* [1985], who used an analytical model of the interaction to correct the phase values. This approach has not been feasible for the antenna array used in this study. Random errors arise from a variety of effects, including the uncertainties of measuring the phase difference of stochastic signals, low signal-to-noise ratios, signal decorrelation across the array, etc. Partial analyses of the random errors have been presented by *Hayenga and Warwick* [1981], *Richard and Auffray* [1985], and *Rhodes* [1989]. In addition to limiting the angular resolution of the instrument, the errors have the practical effect of substantially complicating the data analyses.

For the system of this study, *Rhodes* [1989] has estimated the uncertainty of source locations due to the random phase measurement error to be about 1° rms at high elevation angles. The elevation error increases at lower elevation angles as $1/\sin\theta$ due to the geometric projection effect discussed above. Signal decorrelation across the antenna array also increases the phase and angle errors of the long baselines when the radiation is incident along the baseline. For the 4λ baseline of this study, this increases the rms azimuth error by about $\sqrt{2}$ in the worst case.

The interferometer measurements described above locate the centroid of the lightning radiation as a function of time and produce meaningful results only when the lightning radiation is relatively localized or dominated by a localized source. It happens that this is often the case. The high time resolution of the measurements helps in this regard, as does the fact that multiple sources often have substantially different radiation strengths. In the latter case, the phase values "lock" onto the stronger source. When two spaced events of approximately equal strength are active simultaneously, the sources have been observed to alternate between the two channel segments in response to apparent changes in the relative strength of the radiation from each. The single or dominant source assumption breaks down during initial leaders to ground, which radiate simultaneously from different locations over a relatively large region in the vicinity of the leader channels. Simultaneous multiple events could in principle be imaged using aperture synthesis techniques, but the measurements and processing required to do this are currently prohibitive.

Data and Results

In this section we present results obtained from the analysis of two flashes that occurred on August 23 (Day 236), 1988. The first flash was the subject of the earlier study by *Rhodes* [1989]. A preliminary presentation of the results has been made by *Rhodes et al.* [1991]. The observations were made from our research building in Socorro, at an altitude of 1430 m above mean sea level.

Figure 4 shows composite views of selected results for the two flashes. The source locations are shown both in projection and in azimuth-elevation format. Overall time waveforms for the flashes are shown in Figure 5. Flash 153844 (Figures 4a and 4b and Figure 5a) lasted about 1.2 s and began with 360 ms of intracloud activity followed by 5 strokes to ground. Flash 155325 (Figures 4c and 4d and Figure 5b) lasted about 1 s and began immediately with the initial leader to ground; it produced 9 strokes down the same channel. Both discharges went to ground 5 km or more north of the interferometer site and had in-cloud channels which extended toward, overhead, and past the interferometer site. The ground strokes of both flashes were of normal polarity, that is, they lowered negative charge to ground.

Cloud base for each of the flashes was between 20° and 30° elevation along the vertical part of the channel to ground; the channels above this elevation were inside the storm. The discharges are seen to have been substantially branched inside the cloud. Flash 153844 (Figures 4a and 4b) began at the location denoted by the circled region and established channels A-E during the intracloud phase of the flash. The initial leader to ground began adjacent to the flash start point and established the channel followed by subsequent leaders and strokes. The second stroke required two leaders to initiate. The third stroke initiated a continuing current that originated along the D and E branches. Later strokes originated farther along the main channel to the left of the D segment.

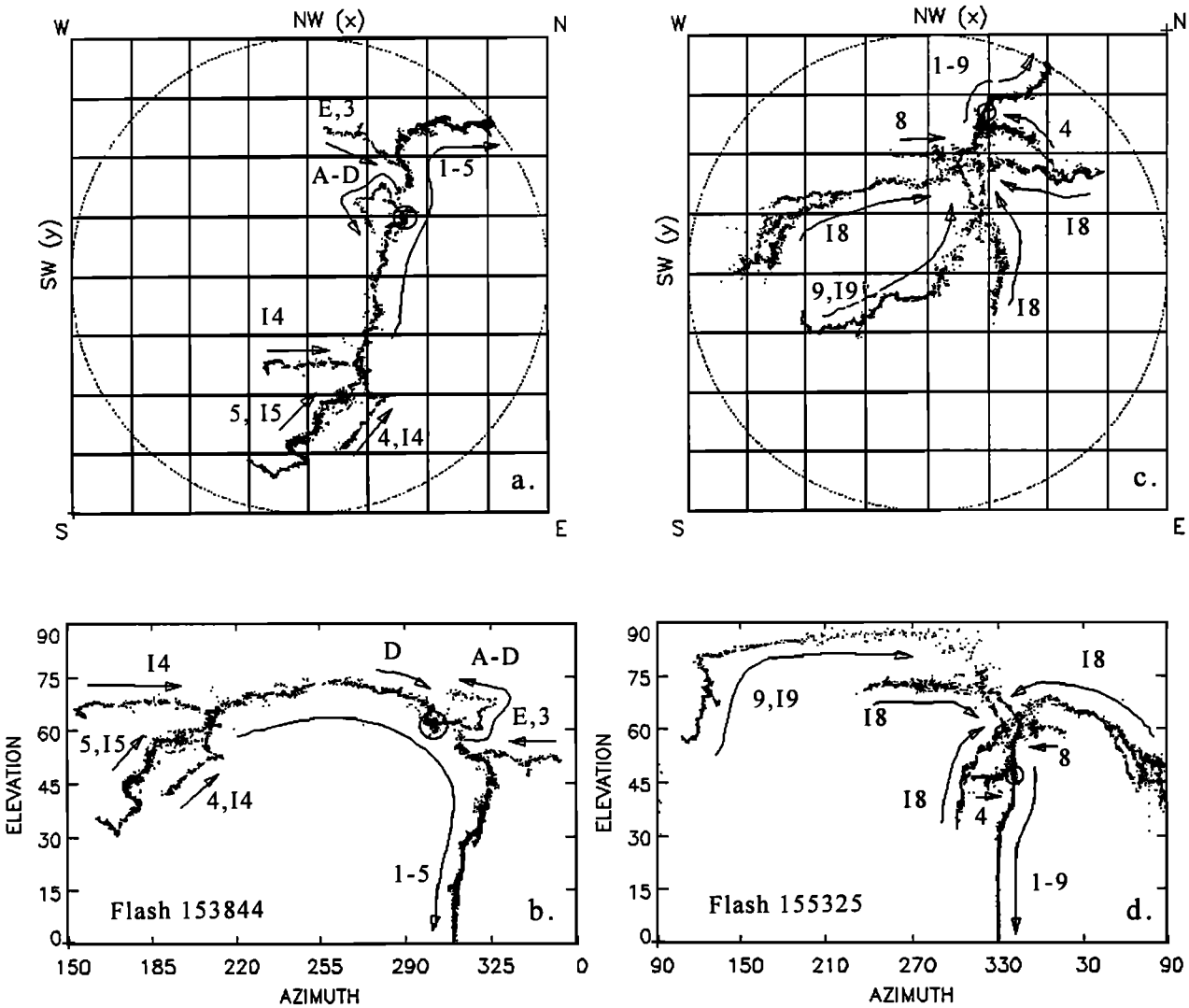

Figure 4. Composite results for flash 153844 in both (a) the projection plane and (b) azimuth-elevation format, showing channels traversed by the preliminary intracloud activity (events A–E), the dart leaders for strokes 3, 4, and 5, and several K streamers in the interstroke intervals following strokes 4 and 5 (I4 and I5). (c), (d) Similar results for flash 155325, showing the dart leaders for strokes 3, 4, 7, 8, and 9, and several interstroke K streamers following strokes 8 and 9 (I8 and I9). Circles indicate the flash starting points.

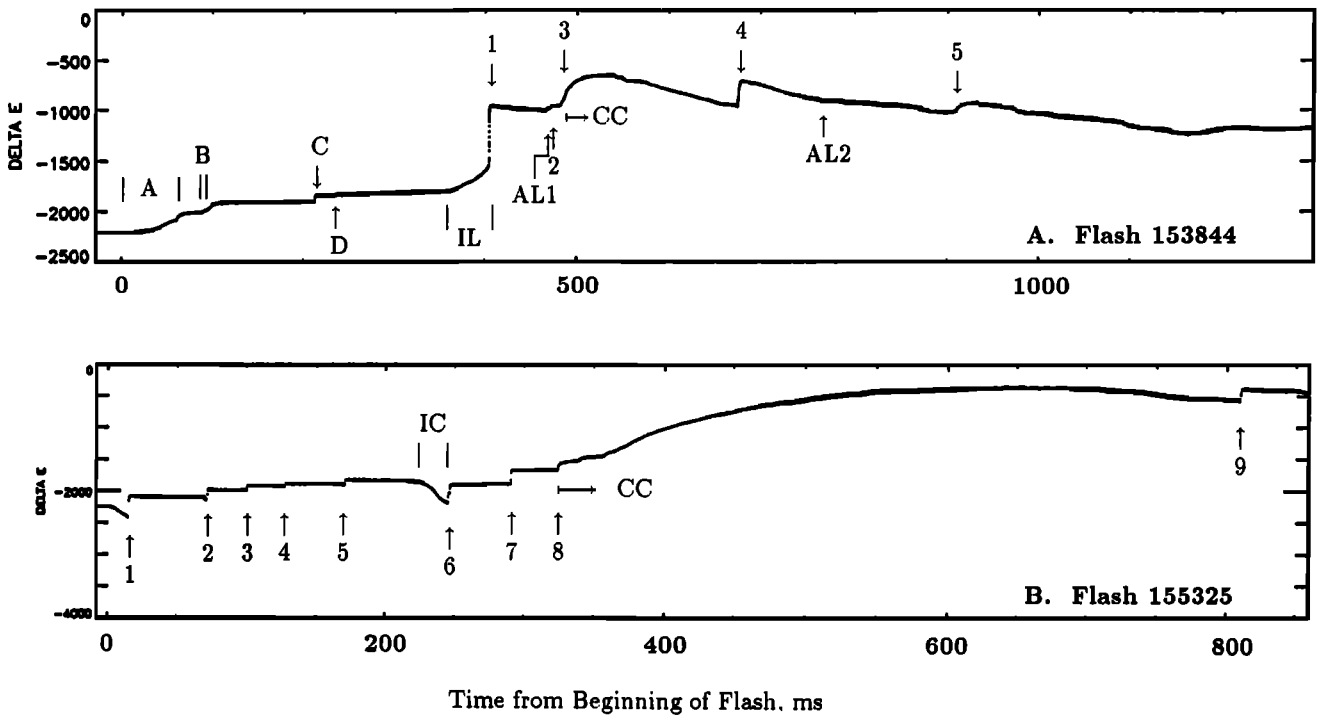

Figure 5. (a) Overall electric field change of flash 153844, showing the time of occurrence of individual strokes (1–5), events of note during the preliminary intracloud activity (A–D), the initial leader (IL) and attempted leaders (AL1 and AL2), and a short continuing current (CC). (b) Same as Figure 6a except for flash 155325, showing the stroke times, the hybrid breakdown event (IC) which initiated the sixth stroke, and the start of a long continuing current.

Flash 155325 (Figures 4c and 4d) produced nine strokes to ground and had a complex structure inside the cloud. Most of the branches were established by intracloud activity late in the flash, after the eighth stroke to ground. The flash started with the initial leader at the circled location in the figures. The leaders for strokes 4 and 8 traveled into the main channel to ground along the short branches near the main channel. The three branches labeled I8 in the figure were traversed only by interstroke activity and K events following the eighth stroke. The long left-most branch was traversed both by the leader for the ninth stroke and by K events subsequent to the ninth stroke. It extended overhead and past the interferometer site; hence its high elevation angle between 210° and 270° azimuth. The branches appear to have extended horizontally in different directions away from the channel to ground, causing the elevation angle of some of the branches to decrease with increasing distance from the interferometer.

The electric field change measurements in Figure 5 were made on the roof our research building and were not calibrated for this study. However, from a previous study the total electric field change of similar flashes in storms in the same area was typically 2.0×10^4 V/m [*Krehbiel et al.*, 1979], within about 10%. Assuming this to be the maximum field change of the flashes in Figure 5 (both of which have about the same total amplitude), we estimate that 100 ΔE units corresponded approximately to 1.0 kV/m electric field change. (This applies to all figures.) The fast ΔE signal was a factor of 12.5 more sensitive; that is, 100 fast ΔE units corresponded to about 80 V/m electric field change. The radiation intensity ("log RF") of later figures is also presented in arbitrary units; for this signal, 24 units corresponded to 10 dB intensity change. The minimum detectable intensity at the receiving antenna (corresponding to a log RF value of about 5 units) was -100 dBm m^{-2} MHz^{-1}.

Initial Breakdown

Flash 153844 began with a long interval of intracloud breakdown that lasted about 360 ms before the initial leader developed to ground. Figure 6a shows radiation source locations for the initial 70 ms of the in-cloud activity, termed interval A in the figure (and in Figure 5a). Radiation during the first 60 ms of A (labeled A1) consisted of a series of bursts whose sources drifted slowly in the direction of increasing azimuth, as indicated by the arrow. During each burst the radiation sources were localized and their extent or motion was not resolved by the interferometer, but the centers of successive bursts were steadily displaced in the direction of progression. The activity culminated with a strong burst of radiation beyond the end of the *A*1 activity, labeled A2.

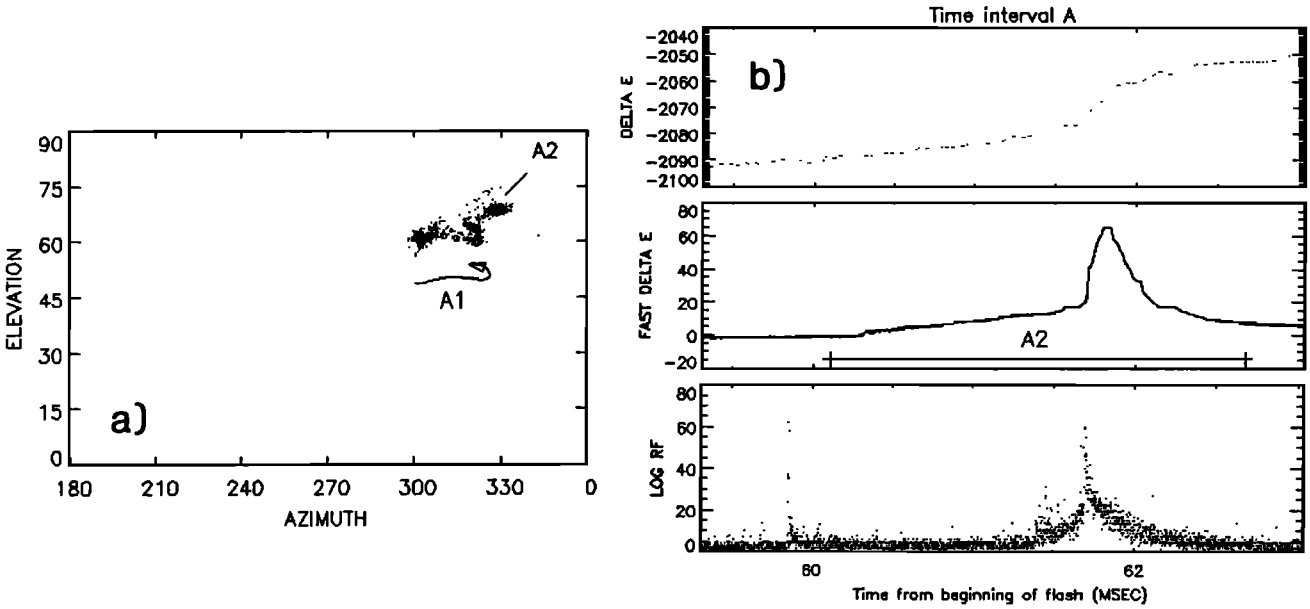

Figure 6. (a) Radiation source locations during the initial 70 ms of flash 153844 (interval A). (b) Expanded time waveforms of the electrostatic field change, fast electric field change, and logarithmic RF radiation amplitude over a 3-ms interval during event A2 at the end of the A activity.

Figure 6b shows expanded time waveforms for the A2 event. The event began with a brief burst of radiation from a localized region just beyond the final A1 sources. The electric field subsequently increased at a steady rate until, 1.5 ms later, additional radiation occurred just beyond the region of the initiating burst. This radiation increased in intensity until a large, rapid electric field change occurred. During this time the radiation sources were displaced away from the location of the initial burst and continued the overall progression of breakdown away from the flash start point.

The electric field change was positive during the entire A event, indicating that negative charge was transported away from the observation site or, equivalently, that positive charge was transported toward the site. Later results presented for the flash show that the A activity progressed away from the observation site; the activity therefore transported negative charge in its direction of progression. The rapid field change during the A2 interval signaled a sudden increase in current, presumably along the full extent of the A channel. (The decrease in the signal following the fast electric field change in Figure 6b was due to the 0.1-ms decay time constant of the fast field change measurement.)

Assuming that the preliminary activity was 5-6 km above ground level, as found by *Krehbiel et al.* [1979] in a similar storm from the same area, and noting that the sources were at about 60° elevation, we infer that the initial activity was about 3 km plan distance from the interferometer. From this and from the angular extent of the source motion, the projected extent of the A progression was about 1 km. The (projected) average speed of progression was therefore about 1.5×10^4 m/s. The three-dimensional extent and speed of progression was greater than this, as the breakdown appeared to be directed mostly away from the interferometer.

K Type Events

Figures 7 and 8 show results for two in-cloud K-type or streamer events which occurred 212 and 231 ms into flash 153844. These events are labeled C and D in Figure 5a. Both retraced the path of the A activity (Figure 6) and successively extended the A path. The first K event (C) is shown in Figure 7. It began with 500 μs of localized radiation in the flash start region (C1) and continued after a 200 to 300-μs lull with a fast streamer (C2), the first well-defined streamer of the flash. The C2 streamer rapidly retraced the path of the A activity and extended the far end of the channel upward in elevation and then backward in azimuth. The electric field increased continuously during the C2 streamer progression, again indicating the transport of negative charge away from the interferometer. As the streamer reached the end of its extent, the radiation abruptly dropped in amplitude and the fast electric field signal saturated. Lower-amplitude radiation persisted for about 100 μs at the far end of the streamer path, then a final burst of radiation (C3) progressed backward along the middle, vertical part of the streamer channel. The entire event lasted about 1 ms, typical of K events.

K event D occurred after a quiet interval of 19 ms and is shown in Figure 8. A brief precursor event, D0, occurred some distance to the left of the previous activity and propagated a short distance toward the flash start point. Then, 4 ms later, a more intense burst, D1, started just beyond the stop point of D0 and progressed

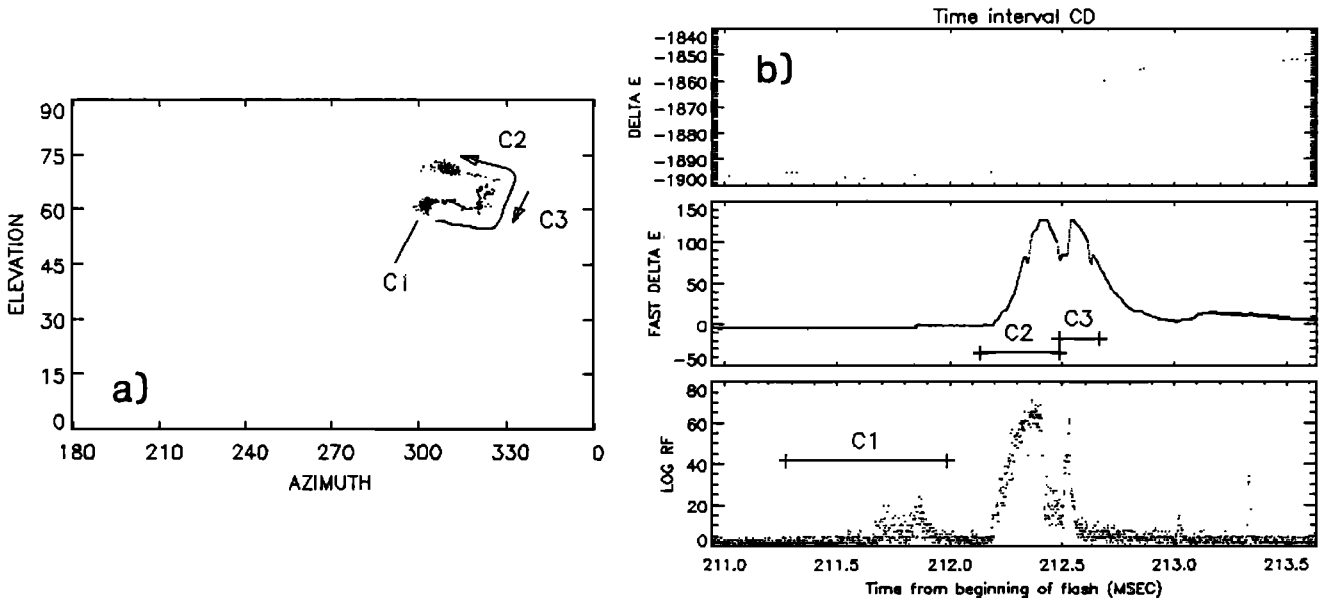

Figure 7. Radiation source locations and time waveforms for K event C of flash 153844, 212 ms into the preliminary intracloud activity of flash 153844.

a slightly greater distance toward the flash start point. About 500 μs later, streamer D2 was initiated at the stop point of D1 and progressed rapidly into the flash start point and without pause along the full extent of the C channel. When D2 reached the end of its extent, a fast field change occurred, signifying a rapid increase in current along the channel, and the radiation abruptly dropped in amplitude.

Event D enables the polarity of the streamers to be clearly established. As will be seen later, the channel extension to the left of the flash start point (D0, D1, and the initial part of D2) was traversed in the same direction by negative polarity dart leaders later in the flash. The electric field change of the dart leaders had the same polarity as the D streamers, indicating that the C and D streamers (as well as the A activity) were also of negative polarity. Each produced a positive field change, implying that they progressed away from the interferometer site. The fact that the elevation angle of the streamers increased at their far end therefore indicates that they developed vertically upward in the cloud or had an upward component. The alternate possibility, that the elevation increase was caused by horizontal motion toward the interferometer, would have produced a field change of the opposite polarity.

Assuming that the total length of the C streamer was 3-4 km, its velocity is inferred to have been $1.5-2\times10^7$ m/s, several orders of magnitude greater than the pro-

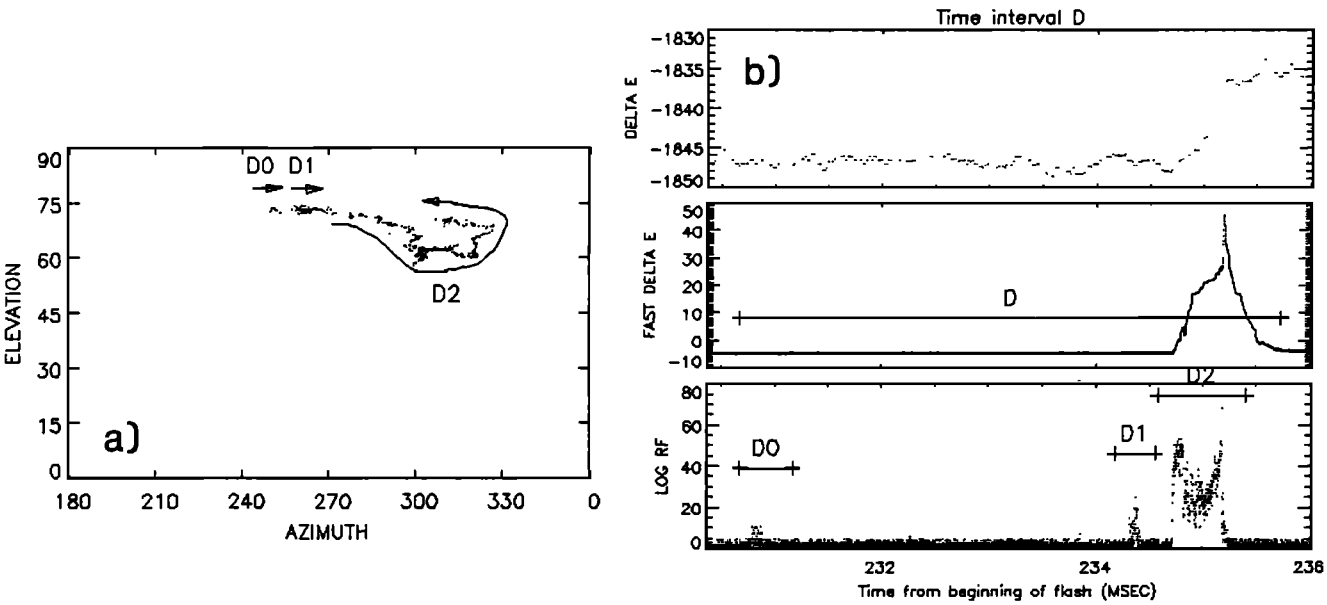

Figure 8. Radiation source locations and time waveforms for K event D of flash 153844, 19 ms after event C of Figure 7.

gression speed of the initial A activity. The D streamer propagated over approximately twice the distance of the C streamer in about twice the time (500 μs), giving a similar speed estimate.

Event D is significant for another reason. A careful analysis of the observations indicates that radiation was not detected prior to the D activity along the channel extension established by D0, D1, and the initial part of D2. Thus the channel appeared to be extended by breakdown which began at a distance from previously detected activity, and the resulting streamer was fast even though no prior radiation was detected along the first half of its path. It is also significant that two precursor events were required to initiate the final D streamer. Each is presumed to have enhanced the local electric stress for the subsequent event.

Initial Leader and Return Stroke

Figure 9 shows time waveforms and radiation source locations for the initial leader to ground of flash 153844. The leader began about 360 ms into the flash and lasted 50 ms. It began abruptly with intense, localized bursts of radiation that commenced in the region labeled S (leader start region). S was close to but in a distinctly different location from the flash start point. The sources progressed slowly but steadily away from S along a relatively well-defined channel. As during the initial breakdown of Figure 6a, the extent or motion of the sources was not resolved during a given burst but the sources progressed to the right and downward from burst to burst. About halfway through the leader, when the sources had descended to about 30° elevation, the bursts increased in frequency and the radiation became continuous and more widespread. The radiation continued in this manner, increasing in intensity, until the leader reached ground. The increased spread of the radiation sources below 30° elevation is indicative of branching, which is confirmed by results for subsequent strokes of the flash (see later Figures 13b, 14b, and 14c).

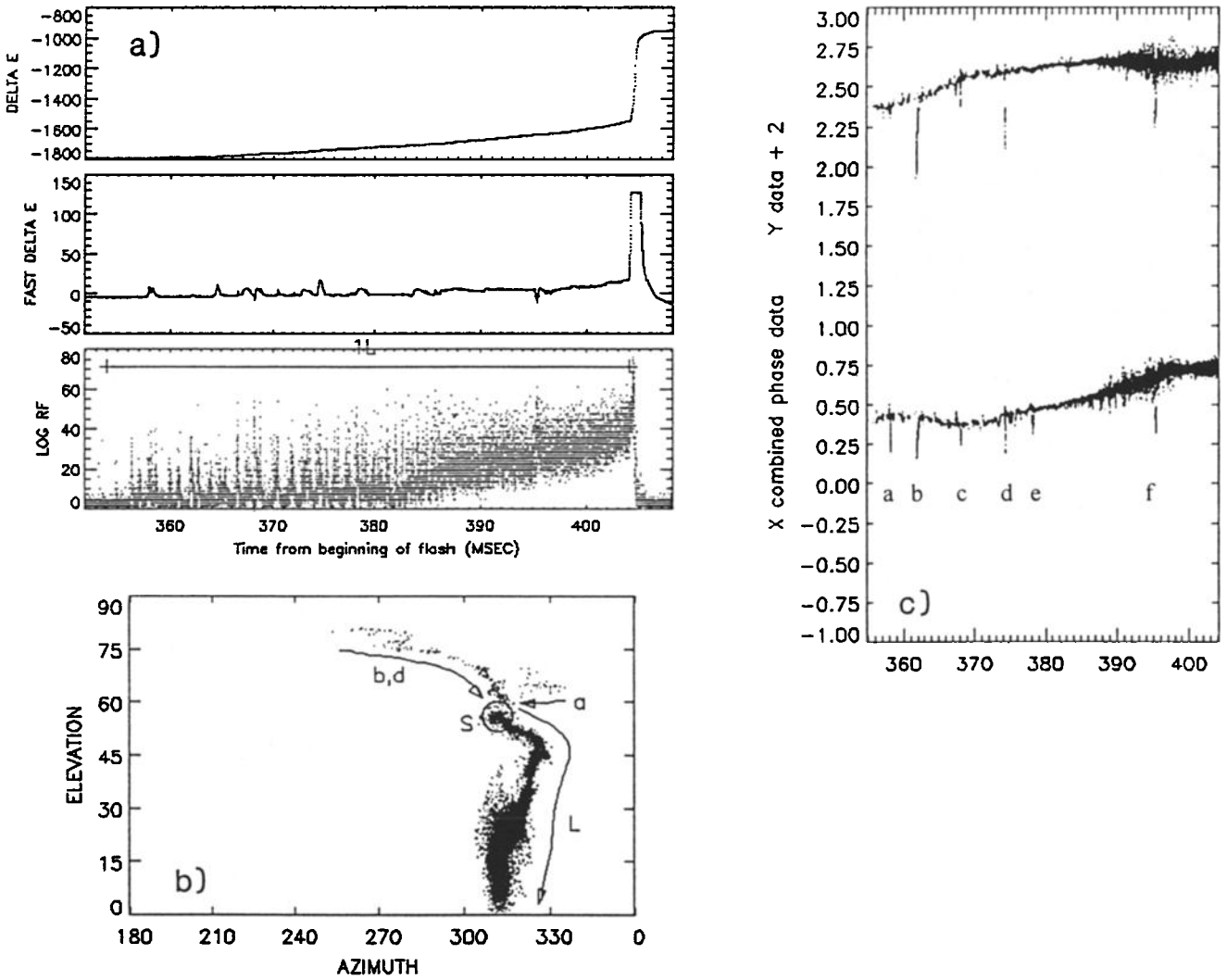

Figure 9. Results for the initial leader to ground of flash 153844. (a) Time waveforms, (b) radiation source locations, and (c) phase values versus time, showing the times of fast streamer events into the leader channel (a–f). The circled region S in Figure 9b indicates the starting point of the leader.

An interesting finding is that several fast streamers occurred during the initial leader. Three of these are shown in Figure 9b, labeled *a*, *b*, and *d*. Each began beyond the starting point of the leader and progressed rapidly into the start region along one of two branches that were established during the preceding intracloud activity. (We refer to these as the left and right branches of the flash (see Figure 4b)). The streamers occurred mostly during the first half of the leader (Figure 9c). They transported negative charge into the developing leader and undoubtedly aide it continued development.

The leader traveled an estimated 5 to 8-km distance in 50 ms, corresponding to an average speed of progression of about 1–1.6 $\times 10^5$ m/s, typical of initial leaders. Although initial leaders propagate in a stepwise manner to ground, no evidence of stepping could be detected in the 1-μs sampled radiation or electric field data. At the close range of the flash, the electric field change is dominated by the electrostatic component, whereas the radiation component is most useful in detecting stepped breakdown. Thus it cannot be determined if the leader began with the characteristic stepping of initial leaders or if stepping developed at a later stage of the leader. The radiation amplitude signal in Figure 9a had a characteristic waveform that is typical of initial leaders, in which the radiation was intermittent during the first half of the leader and became continuous and increased in amplitude as the leader progressed [e.g., *Rhodes and Krehbiel*, 1989].

Figure 10 shows time waveforms and radiation source locations during the final 500 μs of the initial leader through the ensuing return stroke. The electrostatic field change shows that the return stroke lasted about 0.6-0.7 ms and indicates that it had several components. Immediately prior to the rapid field change of the return stroke, a slower precursor change occurred in the fast field record. Expanded time plots show that the precursor change lasted 20 μs. The precursor is believed to

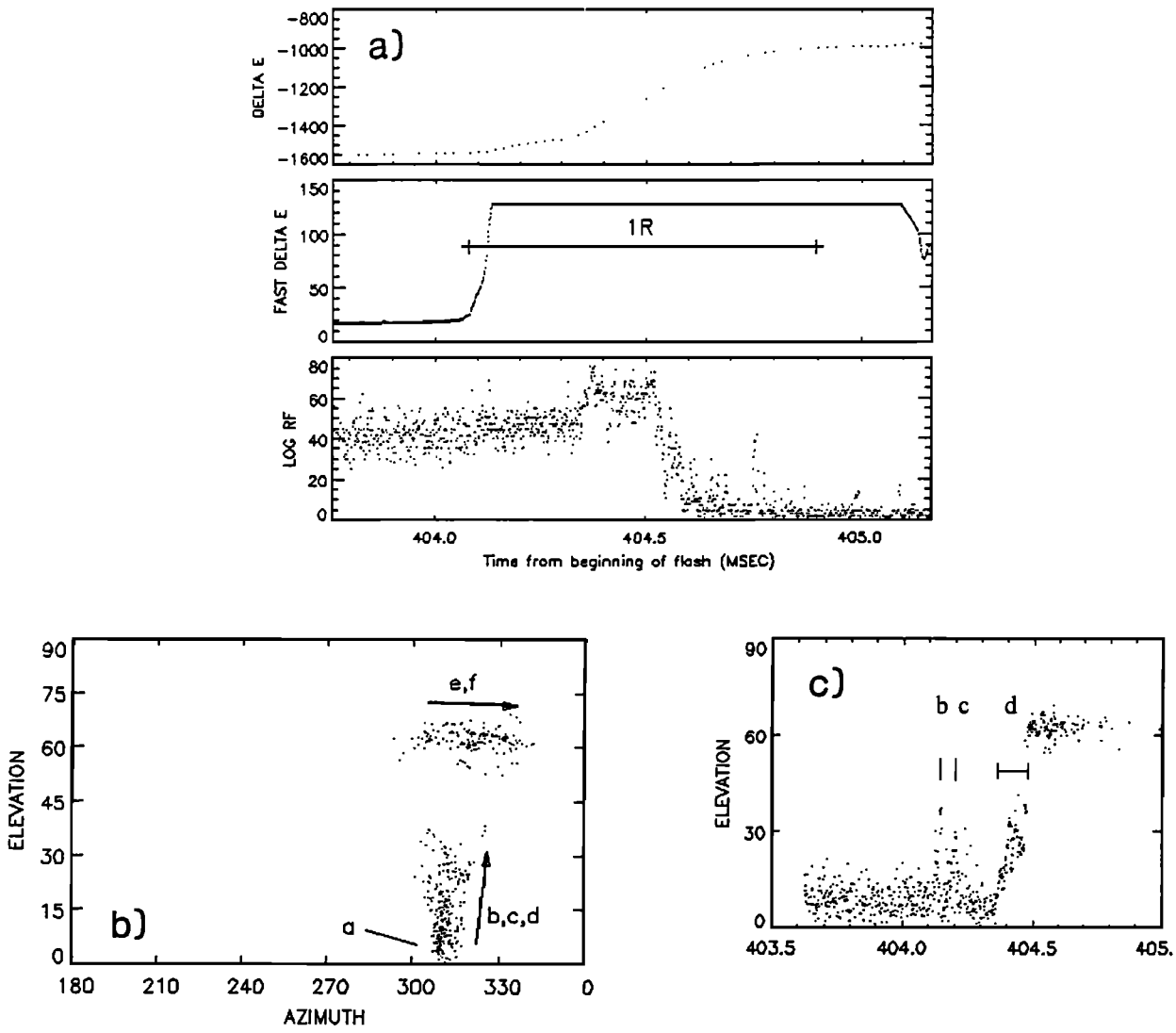

Figure 10. Radiation during the initial return stroke of flash 153844. (a) Time waveforms, (b) radiation source locations, and (c) elevation angle of the sources versus time, showing the time variation of the upward going radiation at the beginning of the return stroke.

have been caused by an upward moving streamer from the ground that completed the connection to ground. The ensuing return stroke quickly saturated the fast field change signal but, as seen on the less-sensitive electrostatic record, initially produced a relatively small electrostatic field change. The return stroke field change intensified 200 μs later, coincident with a noticeable increase in the radiation intensity.

At the beginning of the return stroke the amplitude of the radiation did not change significantly from that of the leader. The radiation source locations during the first part of the return stroke indicate that a sequence of two events (*b* and *c*) traveled up along the lower part of the channel. These are seen between 404.1 and 404.2 ms in the elevation-time plot of Figure 10c and corresponded to the smaller-amplitude initial return stroke. The more intense stroke occurred just after 404.3 ms and was accompanied by stronger radiation that moved rapidly up the lower part of the channel (*d*). The radiation moved up to about 30° elevation, or several kilometers distance, in about 100 μs, corresponding to a speed of about 3×10^7 m/s. (Upward events *b* and *c* were faster than this, on the order of 10^8 m/s.) Subsequently, the radiation abruptly switched to higher elevation and progressed to the right along the right-hand feeder channel of the leader (*e* and *f*). No radiation was detected along the upper half of the leader channel. The concentrated sources labeled *a* at the bottom of the channel in Figure 10b were produced during the final part of the leader. No source motion could be detected during the 20-μs connection event.

Dart Leaders and Return Strokes

Figure 11 shows results obtained for the fourth stroke to ground of flash 153844, which was initiated by a dart leader. (Data for this leader were used to illustrate the phase combination process in Figure 3.) Time wave-

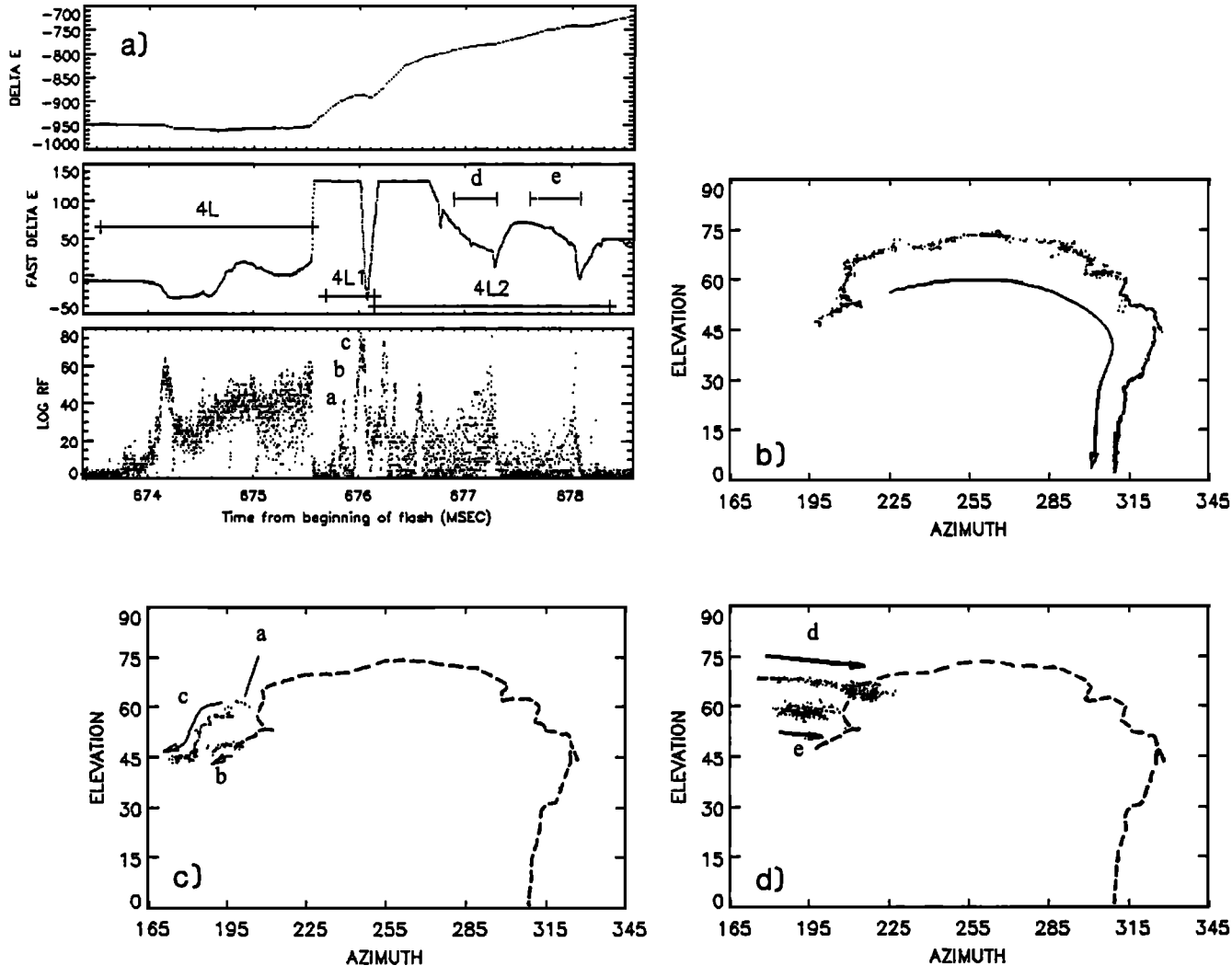

Figure 11. Results for the fourth stroke of flash 153844. (a) Time waveforms, (b) radiation source locations for the dart leader (interval 4L), (c) three positive breakdown events/streamers during the 500-μs time interval immediately following the return stroke (interval 4L1), and (d) two negative streamers which initiated M events down the channel to ground (events d and e, interval 4L2). (The field change of the M event immediately follows each streamer.)

forms over a 5-ms time interval from the beginning of the leader through the resulting return stroke are shown in Figure 11a. The dart leader, shown in Figure 11b, radiated strongly at its advancing tip and progressed continuously along a well-defined path to ground. The leader required 1.7 ms to reach ground and propagated over a substantial horizontal distance within the cloud before turning vertically downward. The final third of the leader was along the path of the initial stroke. The leader began south of the interferometer and propagated overhead and to the north, reaching a maximum elevation of 75° while passing overhead. When the leader sources reached 0° elevation, a fast electric field change occurred indicating the onset of the return stroke, and the radiation abruptly dropped in amplitude. The return stroke saturated the fast field signal but not the electrostatic field change.

Little or no radiation was produced by the return stroke until 200 μs into the stroke, when the first of three radiation bursts occurred, each more intense than the previous (interval 4L1 in Figure 11b). The bursts originated just beyond the initiation point of the dart leader, as shown in Figure 11c. Bursts *b* and *c* were produced by fast streamers that progressed away from the far end of the dart leader along two separate channels or branches. Burst *a* was localized at the start point of *c*. Burst *c* produced a strong negative field change which brought the fast electric field signal temporarily out of saturation. This and the fact that *c* propagated in the opposite direction from the leader (away from the observation site) indicate that it was a positive streamer. Although the fast electric field signal did not come out of saturation during *b*, the fact that it propagated away from the leader indicates that it also was a positive streamer. The time delay of the events after the onset of the return stroke indicates that they were associated with the arrival of the return stroke back in the source region of the dart leader. Careful analysis has shown that no radiation occurred along the *b* or *c* branches prior to the occurrence of the leader. This suggests that their channels were formed by the postive streamers. As we later show, the *a-c* branch was traversed by the final stroke of the flash.

Figure 11d shows radiation source locations for the remainder of the stroke (interval 4L2 in Figure 11b). For about 2 ms following the 4L1 bursts, several negative streamers progressed along two other branches that connected into the channel of the dart leader and return stroke. These branches had been active during the interstroke interval between the third and fourth strokes. The last two streamers are labeled *d* and *e* in the figure and initiated fast electric field changes that are characteristic of "M" components, that is, enhanced current or charge flow down the channel to ground. The M field changes were initiated when each of the streamers appeared to reach the leader channel, at which point the radiation amplitude abruptly dropped. The ensuing M field changes were initially negative and then positive, indicating that negative charge initially approached and then receded from the interferometer site, consistent with the fact that the channel passed over the interferometer. The continued positive fast field change indicates that the charge went all the way to ground and was part of a short continuing current. The fact that no radiation was detected along the main channel during the return stroke or during the M events is typical of conducting channels and illustrates that radio frequency radiation is produced by the breakdown of new or decayed channels rather than by current flow along already conducting channels.

The total length of the fourth stroke leader is estimated to have been about 20 km, corresponding to an average speed of about 1–1.5 $\times 10^7$ m/s. This is similar to the K streamer speeds during preliminary breakdown. The quiet period following the onset of the return stroke lasted 200 μs; assuming this to be the time required for the return stroke to arrive back in the leader source region, the average speed of the return stroke was about 1×10^8 m/s.

Figure 12 shows results for the fifth and final stroke of flash 153844. The leader for the fifth stroke was initiated 220 ms after the fourth stroke and required a relatively long time (14 ms) to reach ground. The leader traveled rapidly (about 10^7 m/s) until reaching its approximate midpoint overhead of the interferometer, and then progressed more slowly (less than 10^6 m/s) and with increased radiation intensity to ground. The leader started slightly beyond the channel established by the positive *a–c* streamer at the end of the fourth stroke. (This channel had been retraced and extended numerous times during the interstroke interval leading up to the fifth stroke). The fifth return stroke was less intense than the fourth return stroke and did not saturate the fast electric field signal. It was accompanied by a quiet period of about 1-ms duration in the radiation amplitude and then by a single burst of radiation back in the source region of the leader (interval 5L1 of Figure 12a, and Figure 12c). Like the bursts following the fourth stroke (Figure 11c), this burst was a positive streamer. Rather than extending the leader channel, however, as in the fourth stroke, the fifth stroke streamer retraced the initial part of the leader. The long duration of the leader apparently had allowed its initial segment to become nonconductive. Assuming that the positive streamer was launched by the arrival of the return stroke back in the leader source region, the speed of the return stroke was about 2×10^7 m/s or a factor of 5 slower than the fourth, more energetic, leader and stroke.

Continuing Current Event

Figure 13 shows results for the third stroke of flash 153844. This stroke initiated a continuing current discharge to ground of about 60 ms duration. The leader lasted about 2 ms and consisted of an unusually complex sequence of breakdown events along both the left- and right-hand channels of the flash (Figure 13b). The return stroke occurred at the time of the positive step in the fast electric field record (482.8 ms in Figure 13a); following it the electrostatic field continued to increase,

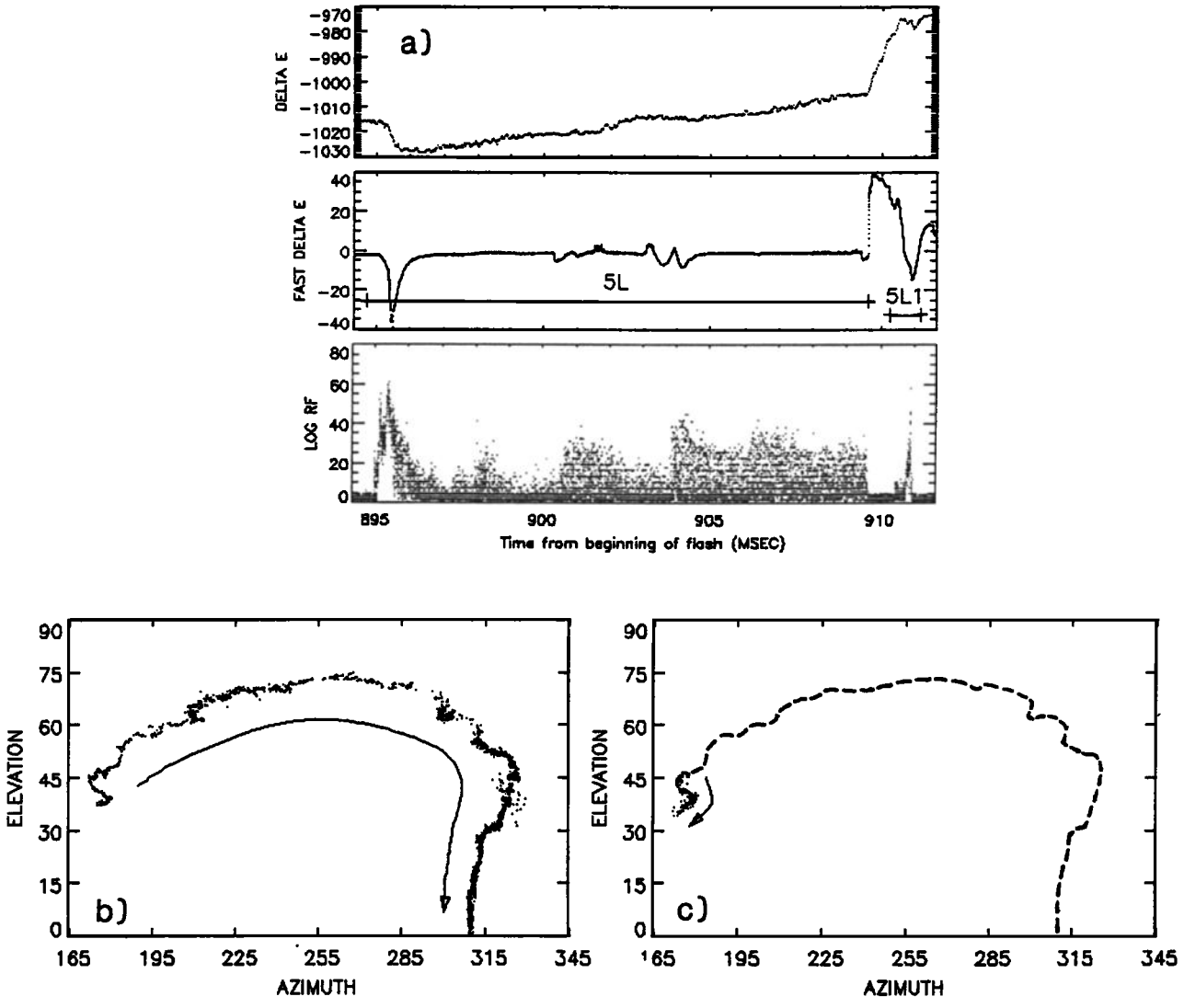

Figure 12. Results for the fifth stroke of flash 153844. (a) Time waveforms, (b) radiation source locations for the dart leader (interval 5L), and (c) positive streamer immediately following return stroke (interval 5L1).

indicating continued flow of current to ground (see also Figure 5a). At the beginning of the return stroke, the radiation signal decreased in amplitude but, unlike strokes 4 and 5, did not become quiet. Rather, radiation was produced at intermittent times and locations from successively higher points along the channel, mostly from apparent branch points as the return stroke traveled up the channel. The return stroke source locations are shown in Figure 10c, adjacent to and along the *e* and *c* segments of the leader channel. Figure 13d shows that the elevation angle of the sources increased linearly with time after the return stroke onset, at a rate of about 20° per 100 μs. Because the downward channel to ground was directed slightly away from the interferometer site, it is estimated to have been approximately equidistant from the interferometer, at a radius of about 6 km. The rate of elevation increase therefore corresponded to an upward speed of 2×10^7 m/s for the return stroke.

Several M events occurred during the continuing current, each of which enhanced the current to ground. The first two M events occurred 1 ms and 10 ms into the continuing current and were initiated by the radiation shown in Figure 10c. In each instance breakdown began just beyond the end of one of the leader branches and progressed into the leader channel. Upon reaching the channel, the breakdown initiated a fast field change characteristic of an M component and renewed the electrostatic field change, indicating increased charge flow to ground. The first event (M1) started about 700 μs into the return stroke and was initiated by breakdown just beyond the *a* region that was active at the beginning of the leader. As for the M events of stroke 4 (Figure 11), the M field change was initially negative and then positive, consistent with negative charge transfer initially toward and then away from the interferometer site. The second event (M2) traveled into and along the right-hand branch, nearly to the junction

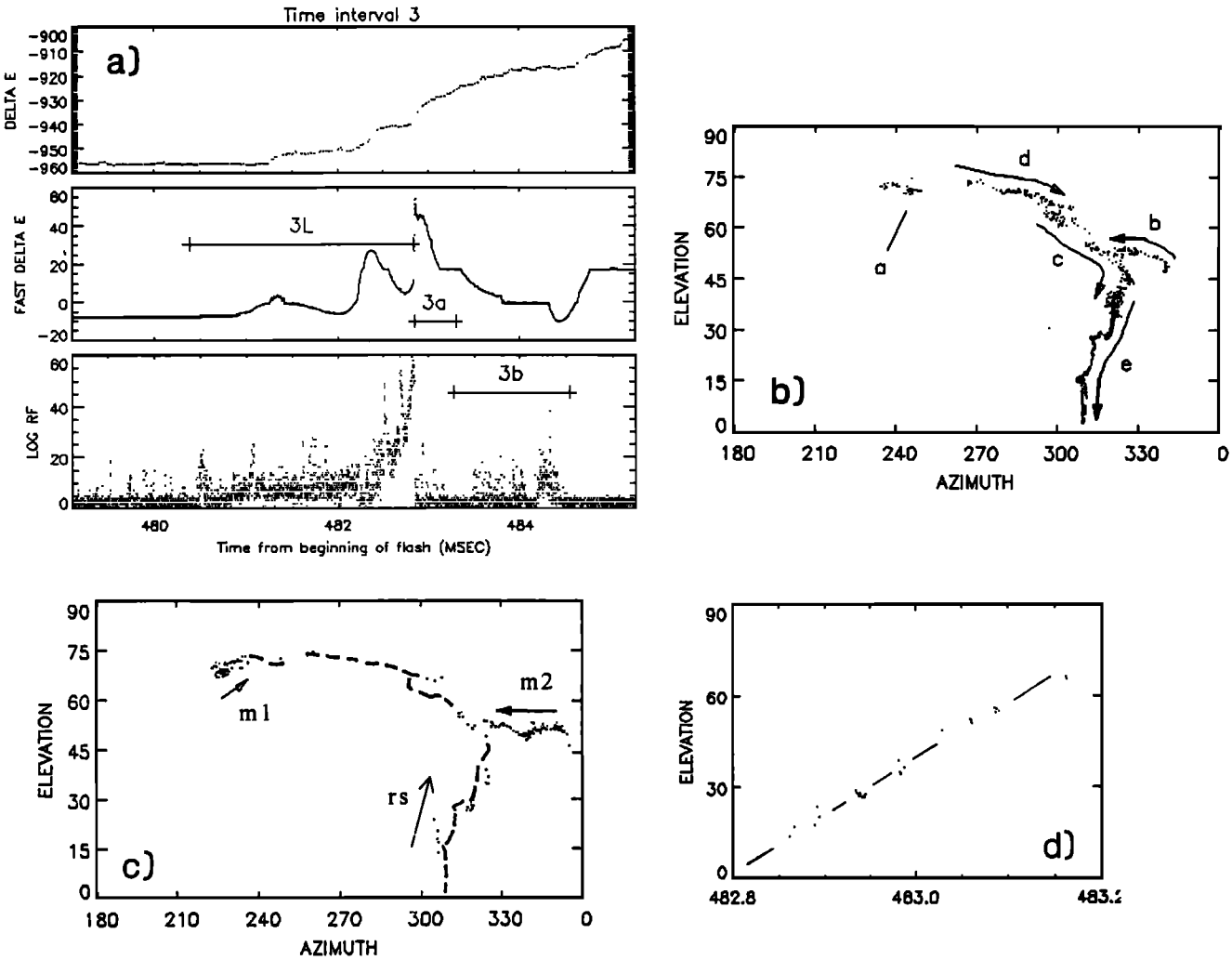

Figure 13. Results for third stroke of flash 153844, which initiated a continuing current discharge to ground. (a) Time waveforms, (b) radiation sequence during dart leader, (c) sources of intermittent, upward-going radiation during the return stroke, and radiation of breakdown which initiated two M-events (m1 and m2), and (d) elevation increase versus time of the upward going return stroke radiation.

point of the branch with the main channel, before initiating the M field change. (Time waveforms for this event are not shown but were similar to those of the first M event. In both instances the radiation amplitude decreased when the breakdown reached the leader channel.) The continuing current therefore appeared to be sustained by charge beyond the end of both branches. Leader branching or complexity is not necessary for a continuing current discharge, as the long-duration continuing current initiated by stroke 8 of flash 155325 was initiated by a normal dart leader.

Attempted or Aborted Leaders

In addition to the initial and dart-type leaders discussed above, flash 153844 produced two attempted leaders which died out before reaching ground. The first attempted leader occurred 62 ms after the initial stroke and was the first of two successive leaders which initiated the second stroke to ground. Time waveforms for the two leaders (labeled 2L1 and 2L2) are shown in Figure 14a. Source locations for the attempted leader (2L1) are shown in Figure 14b, and those for the successful leader (2L2) are shown in Figure 14c. (The two events are labeled "AL1" and "2" in the overall time waveforms of Figure 5a.) Several milliseconds prior to the attempted leader, two radiation bursts occurred along the left-hand channel extension established by K event D (Figure 8). The sources of these bursts are labeled *a* and *b* in Figure 14b. After a delay of 1.5 ms, a dart-type streamer (*c*) began abruptly in the vicinity of the *a* activity and propagated into the start point of the initial leader and along the path of the initial leader toward ground. (The path is also the same as that for the leaders of strokes 4 and 5, shown in Figures 11 and 12.) The *c* streamer traveled an estimated 6 to 7-km distance in 1.5 ms down to about 10° elevation, corresponding to an average speed of about 4×10^6 m/s. At this point the fast motion stopped and radiation switched back up to about 30° elevation, slightly to the left of the *c* path, and descended slowly toward ground along a separate

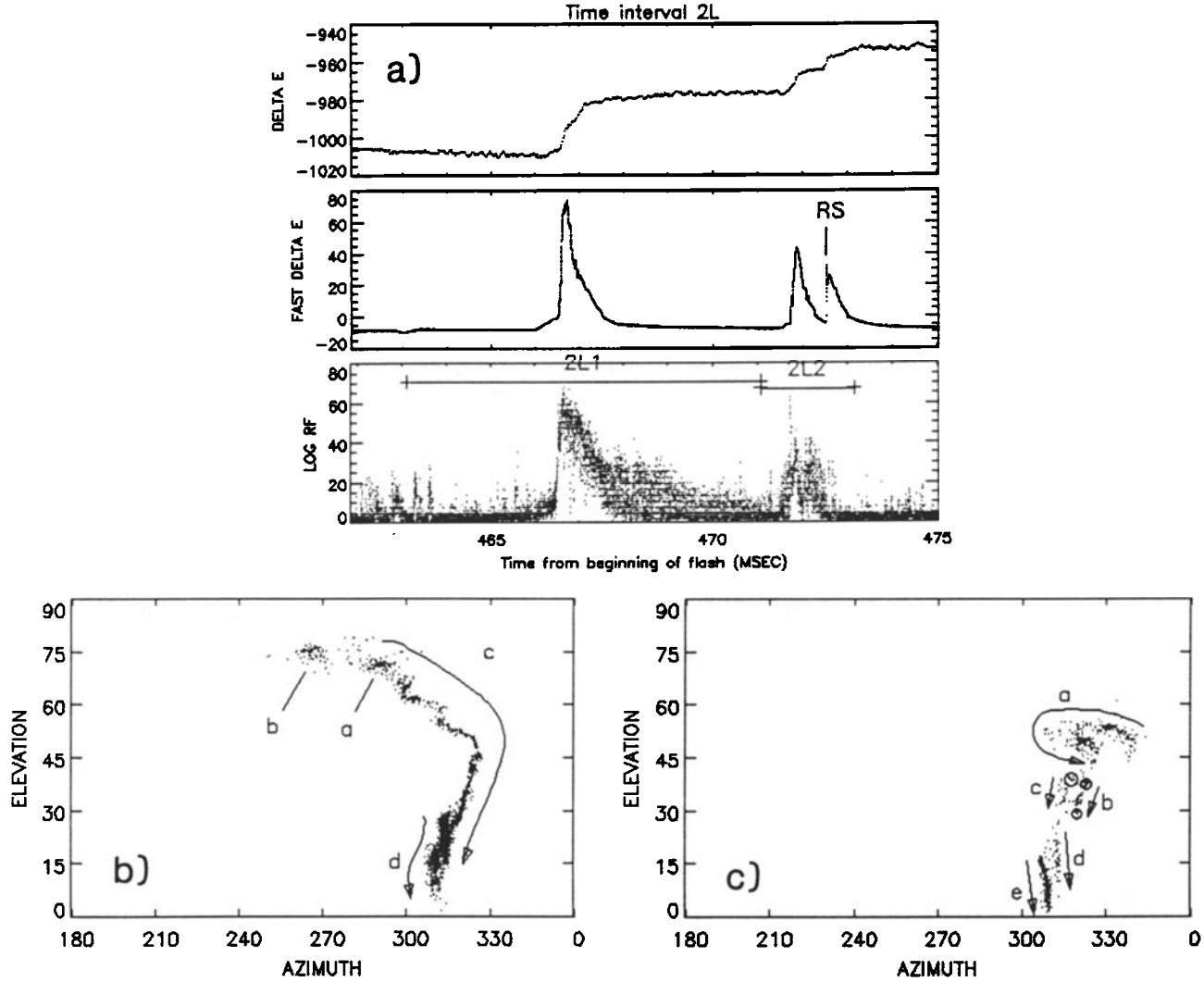

Figure 14. Results for the attempted and successful leaders of the second stroke to ground of flash 153844. (a) Time waveforms for the two events. The return stroke is labeled RS. (b) Radiation sources for the attempted leader (2L1). (c) Radiation sources for the successful leader (2L2). The small circles indicate the sources of impulsive radiation during the return stroke.

path (*d*). Although not fully evident in Figure 14b, time animation shows that the *d* channel was distinctly different than the lower part of the *c* channel. The *d* descent lasted for about 3 ms, between 468 and 471 ms in Figure 14a, during which time the radiation was impulsive and steadily decreased in amplitude. The fact that it did not reach ground is evidenced both by the source locations and by the lack of a step return stroke change in the fast electric field record.

As the first leader died out, the second leader (2L2) occurred which succeeded in reaching ground and initiated the second stroke. The leader began 5 ms after 2L1 (just before 472 ms in Figure 14a) and reached ground in about 1 ms. It began along the right-hand branch of the flash and progressed slowly along a spatially noisy path (*a*) into the main channel and then rapidly toward ground (*b–d*). During its descent, radiation was produced only along intermittent segments of the channel, indicating that the channel remained conductive from the attempted leader. The final connection to ground, *e*, extended path *d* of the attempted leader and required 0.5 ms to bridge the remaining gap to ground. The return stroke occurred at the time of the final, fast positive field change (RS in Figure 14a). The previous two field changes in the fast ΔE record were produced by the leaders. Although the electrostatic field change of the attempted leader (top panel of Figure 14a) resembled that of a successful stroke to ground, only the fast electric field waveforms reliably indicate the occurrence of a stroke. The small circles in Figure 14c indicate the sources of three radiation bursts which occurred at successive 50-μs intervals after the start of the return stroke. In time sequence, the bursts originated at the upper end of the *c* segment and at the lower and upper ends of the *b* segment. The first two locations corresponded to the ends of apparent branches, while the third appeared to lie on the main channel.

Figure 15 shows results obtained for the second attempted leader of flash 153844. This occurred 86 ms after the fourth stroke to ground, partway through the

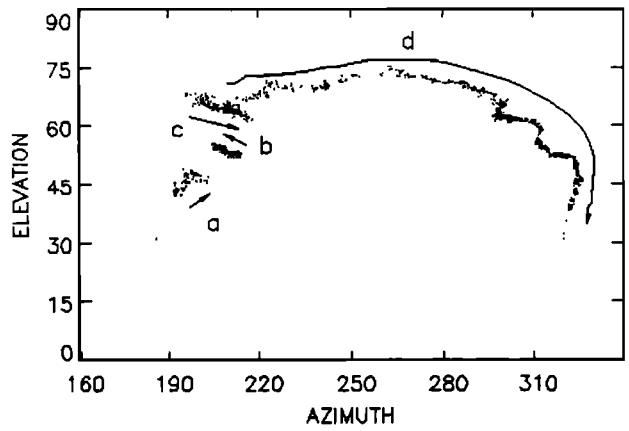

Figure 15. Radiation source locations for an attempted leader that occurred halfway through the interstroke interval between the fourth and fifth strokes of flash 153844.

interstroke interval between the fourth and fifth strokes. (This event is labeled AL2 in the overall time waveforms of Figure 5a). Several disjoint radiation events (a–c) were followed by a negative streamer (d) which retraced the path of the fourth stroke leader before dying out part way down the vertical channel to ground. The streamer traveled an estimated 5 to 10-km distance in 2 ms, corresponding to an average speed of $2.5–5 \times 10^6$ m/s. Except for its large extent, d behaved identically to the streamers of K type events that were occurring in the interstroke intervals. This, and the obvious similarity of d to a dart leader, demonstrates that there is essentially no difference between K events and dart leaders, except that the latter have enough energy to reach ground.

Additional Dart Leader Results

We turn now to the second of the two flashes, flash 155325, and briefly document two features of this flash that differed from those observed in flash 153844. The first feature concerns a different type of post dart leader radiation. Figures 16a–16c show results obtained for the third stroke to ground, which was initiated by a dart leader. The leader began with localized, stationary radiation at the top of its channel, then progressed rapidly to ground along a well-defined path (Figure 16b). It traversed an estimated 5-km distance in 300 μs, corre-

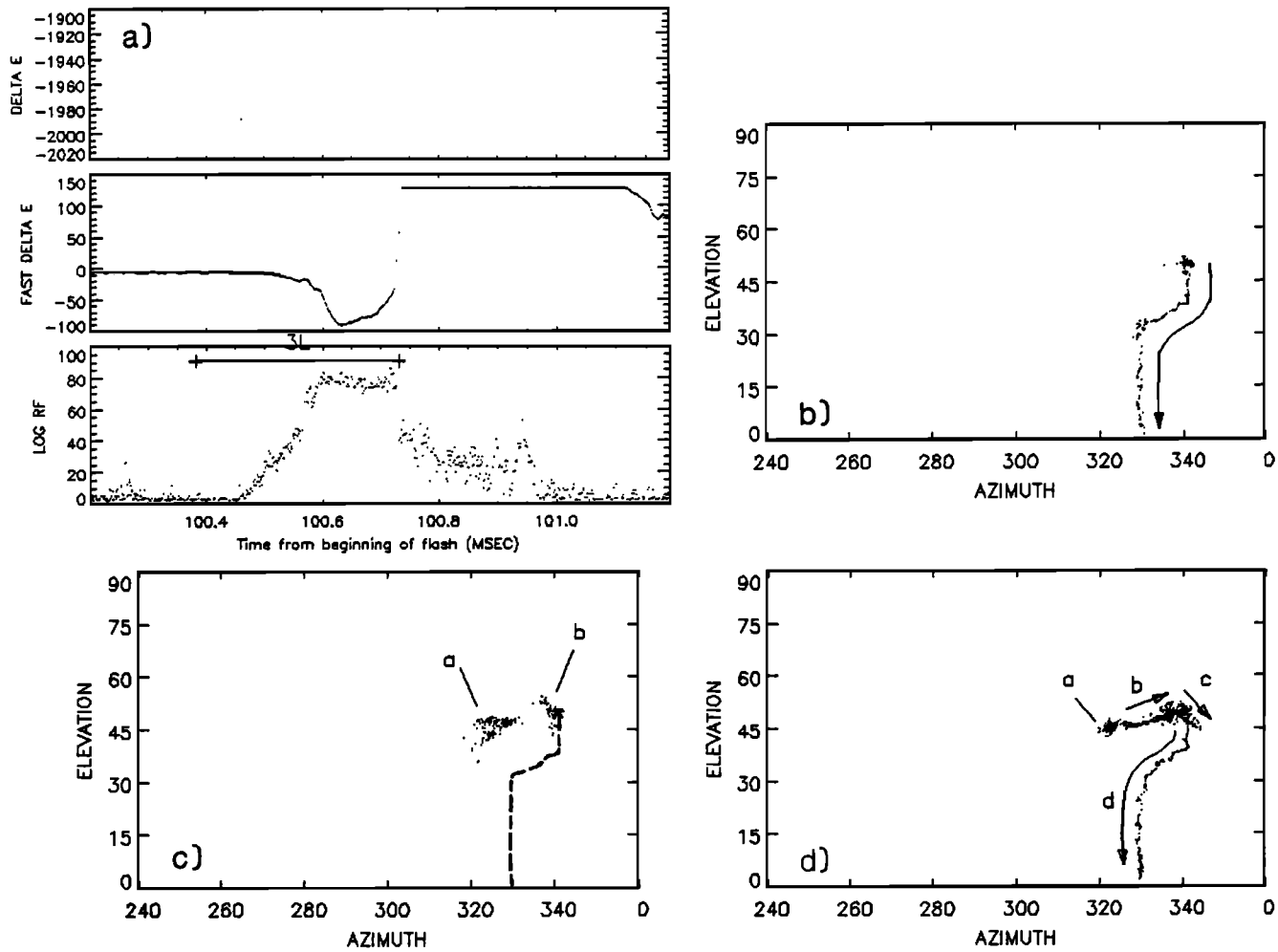

Figure 16. Results for the third stroke to ground of flash 155325. (a) Time waveforms, (b) radiation sources of the dart leader, (c) post leader radiation sources (a: breakdown revealed by cessation of dart leader radiation; b: delayed radiation associated with arrival of return stroke at top of leader channel), and (d) leader for next (fourth) stroke of flash.

sponding to an average speed of about 1.5 $\times 10^7$ m/s. At the onset of the return stroke, the radiation dropped abruptly in amplitude, but not down to the receiver noise level, as it did for the later strokes. Rather, the radiation continued at a lower level through the time of the return stroke. (The radiation waveform shown in Figure 16a is the output of a logarithmic receiver, so that the decrease at the time of the return stroke was substantial, about 15 dB.) The continuing radiation originated from the region labeled *a* in Figure 16c. It occurred at the same elevation as the source region of the dart leader, but was displaced from the source region. The *a* radiation continued for 150 μs until about 100.9 ms, when two large-amplitude bursts occurred at the upper end of the leader channel, labeled *b* in Figure 16c. The time delay and location of the *b* events suggest that they were associated with the arrival of the return stroke at the top of the leader channel. Assuming this to be the case, the average speed of the return stroke was about 3 $\times 10^7$ m/s (only twice as fast as the leader speed).

The result that the radiation immediately following the leader shifted location to region *a* and was reduced in amplitude indicates that the *a*-breakdown was concurrent with that of the downward progressing leader but was not revealed until the more strongly radiating leader was extinguished. No direction of progression could be discerned during the *a* activity, as the source locations were randomly located with time. Also, no activity was detected in the *a* region prior to the third stroke. However, the *a* region became the starting point of the leader for the next stroke of the flash, shown in Figure 16d. This suggests that the concurrent leader breakdown was responsible for establishing this branch of the flash. As can be seen in the overviews of Figures 4c and 4d, the flash was highly branched inside the cloud. Similar breakdown was found to accompany most of the leaders of the flash and appeared to intitiate most of the branches.

A New Type of Hybrid Breakdown Event

Figure 17 shows results obtained prior to the sixth stroke to ground of flash 155325. The electrostatic field change prior to the return stroke resembled that of an initial leader to ground, in that it was long in duration and increasingly negative leading up to the return stroke (IC in Figure 5b and 6L in Figure 17a). But the radiation sources show that the breakdown progressed horizontally through the cloud rather than to ground (Figure 17b). Widespread and continuous radiation began at an intermediate elevation angle in the vicinity of the earlier channels to ground and progressed slowly and continuously away from the earlier channels toward and past the interferometer along an apparently horizontal path. The sign of the electric field change indicates that the breakdown transported negative charge in its direction of progression, and was therefore of negative polarity.

After 60 ms of the above activity a dart leader originated back in the source region of the breakdown that progressed rapidly in the opposite direction to ground. The dart leader was also of negative polarity, and its occurrence terminated the slow activity. Both the slow activity and the stroke to ground transported negative charge away from their common source region. We speculate that the slow moving radiation was produced by the highly branched, slow-moving "finger"-type discharges that are sometimes observed to propagate horizontally through the base of older storm complexes

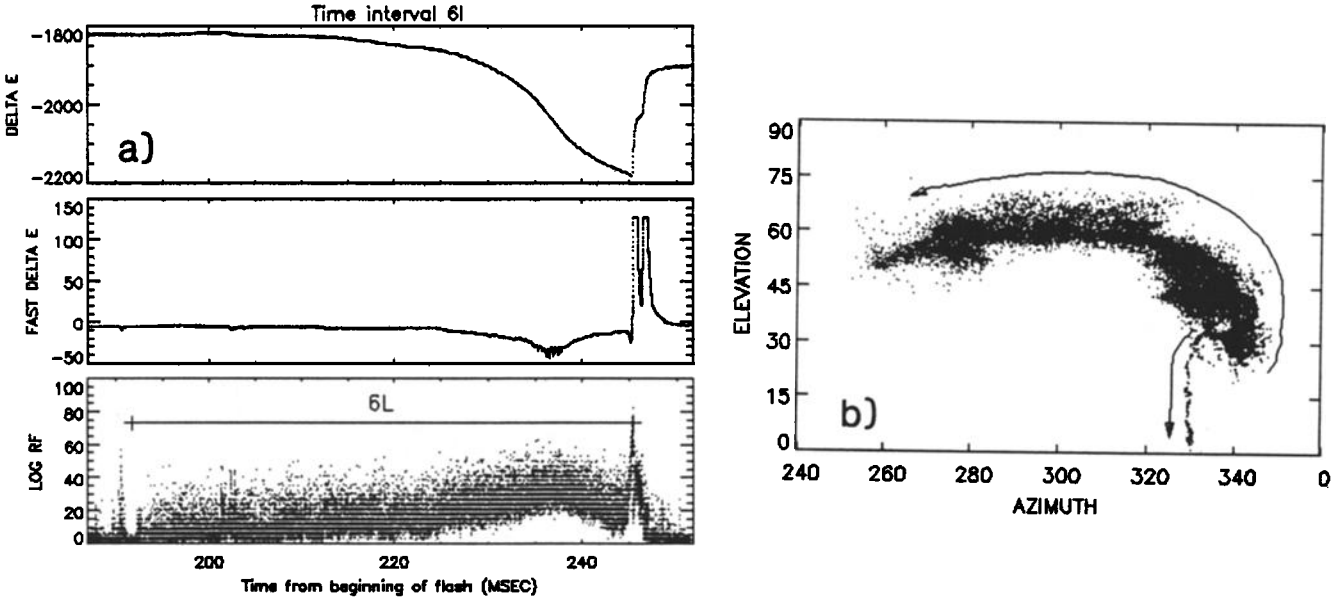

Figure 17. Time waveforms and radiation sources for the hybrid breakdown which preceded and initiated the sixth stroke to ground of flash 155325, showing the extensive horizontal activity which preceded the dart leader to ground.

(e.g., the "air discharges" described by *Malan* [1963], and the "rocket" lightning of *Uman* [1987]). Additional examples are required for a better understanding of this phenomenon.

Summary and Discussion

The results of this study further illustrate the usefulness of interferometric techniques for studying lightning discharge processes. They agree in a number of respects with results obtained from previous studies of lightning radiation but also differ with and/or clarify some previous results. In this section we summarize the discharge characteristics observed in this study and compare them with previous results.

Much of the VHF radiation from lightning occurs in bursts lasting several tens to several hundreds of microseconds or longer. Interferometric techniques enable the radiation sources to be located as a function of time during such bursts. The bursts appear to be produced by two distinct kinds of breakdown events: (1) fast-moving streamers which propagate along well-defined channels during a given burst, at speeds of $1\text{–}2\times10^7$ m/s down to about 10^6 m/s, and (2) localized, intense breakdown whose motion within a burst is not resolved but whose centroid progresses slowly from burst to burst. In both cases, the breakdown is predominantly negative in polarity, that is, negative charge is transported in the direction of the breakdown progression. Radiation is also observed from fast positive streamers, as discussed later.

Fast-moving negative streamers are characteristic of both dart leaders to ground and in-cloud K type events, and appear to be the same process in both instances. As noted by *Hayenga* [1984], the two types of events appear to be distinguished only by the fact that dart leaders develop toward ground and initiate a return stroke, whereas K streamers progress horizontally or upward in the storm. Some K streamers produce fast field changes (e.g., Figure 8), indicative of a rapid current increase along the streamer channel. Many K streamers do not produce a fast field change, however, but simply die out after traveling some distance.

While most dart leaders progress continuously along a well-defined path to ground, the leader breakdown is sometimes complex and involves different branches and channel segments (Figures 13b and 14c). In addition, some dart leaders die out before reaching ground (Figures 14b and 15). These further illustrate the similarity between dart leaders and K events.

Localized, slow-moving radiation is observed during the initial intracloud breakdown of a flash and during initial leaders to ground (Figures 6 and 9, respectively). The speed of progression is estimated to be about 10^5 m/s during initial leader breakdown and greater than 10^4 m/s during initial breakdown of intracloud activity which preceded the cloud-to-ground phase of the flash. Radiation during initial leaders often becomes increasingly widespread with time, which appears to be related to the development of branches. A new type of event has been identified which resembles that of an initial leader to ground, except that it progresses horizontally within the storm rather than going to ground. In the instance reported in this paper, the slow breakdown spawned a negative-polarity dart leader in the opposite direction to ground (Figure 17).

The result that radiation during initial breakdown is localized and slow moving agrees with the observations of other investigators for ground flashes preceded by intracloud activity. In summarizing the results from a number of flashes, *Proctor et al.* [1988, p. 12,709] reported that the noise sources during such activity "clustered in a region about the origin." *Warwick et al.* [1979] reported one-dimensional source locations for one flash that were noisy but drifted at an estimated (projected) speed of 3×10^4 m/s. *Richard et al.* [1986] reported that the initial radiation sources were scattered over distances of about 1 km and in some cases drifted or expanded and spread.

Similar agreement is obtained with previous results concerning initial leaders to ground. *Proctor et al.* [1988] reported speeds of $1\text{–}2\times10^5$ m/s for the radiation sources of initial leaders. He found that initial leaders were easy to map and were often heavily branched and complex. *Hayenga and Warwick* [1981] observed a progression speed of 2×10^5 m/s during horizontal progression of the first 31 ms of an initial leader to ground and 5×10^5 m/s during the downward descent of the leader. *Richard et al.* [1986] were unable to resolve the ambiguities of their 10-λ system during initial leaders because of the large dispersion of the sources but reported a drift speed of about 10^5 m/s during the first 10 ms of a 25-ms initial leader to ground. *Uman et al.* [1978] and *Rustan et al.* [1980] reported a significantly higher speed for the initial leader of an energetic 3-stroke flash which happened to strike a tower. The initial leader required only 4.9 ms to traverse a 7-km distance to ground, corresponding to an overall average speed of about 1.5×10^6 m/s.

During the initial leader of flash 153844, a sequence of fast negative streamers was observed to propagate along earlier channels into the start region of the leader (Figure 9). This is a new result that was missed in the original analysis of the flash but which has since been observed in other flashes and may be commonplace. The fast streamers undoubtedly progress down the developing leader channel and supply negative charge that assists the leader's development. *Proctor et al.* [1988] reported the occurrence of several "exceptional" sources which became active above the leader origin at the end of an initial leader, that may have been produced by the same phenomenon. We have not been able to identify stepping in the initial leaders, either from the radiation signals or from electric field measurements. The latter were dominated by the electrostatic change of the leader at the close range of the measurements. Hence we use the term "initial" rather than "stepped" leader.

The fast streamers of in-cloud K events have been observed by other investigators and are particularly well-delineated by interferometric measurements. *Hay-*

enga [1979, 1984] termed the streamers "fast bursts" and noted their correlation with K events, as well as their similarity with what *Proctor* [1976] termed "Q" noise and with what *Rustan et al.* [1980] termed "solitary pulses." Hayenga found that the fast bursts preceded the K field change and reported one fast burst to have a speed of about 2×10^7 m/s over an estimated length of 6 km. The speed was noted to be one order of magnitude greater than the value of 1.3×10^6 m/s determined by *Ogawa and Brook* [1964]. (Ogawa and Brook's value was based on the assumption that K changes travel over a 1-km distance in about 1 ms and thus was only an estimate.) *Richard et al.* [1986] observed fast streamers during intracloud discharges that traveled distances of up to 10 km at speeds of about 10^7 m/s. These and other fast streamers were observed by them to travel along well-defined channels and to represent a major part of the radiating activity of a discharge. The fast streamers were found to be associated with K type field changes and were considered by *Richard et al.* [1986] to be associated with recoil streamers of the K events. They noted that the speeds were greater than photographic estimates of $1 - 4 \times 10^6$ m/s from *Brook and Ogawa* [1977] and, because of this, concluded that the radiation was decorrelated with the optical K event. Richard et al.'s interpretation that the streamers were recoil events conflicted with Hayenga's observations that the streamers preceded the fast electric field change of a K event.

The K streamers of the present study traveled at speeds similar to those of the above observations, with values ranging from $1 - 2 \times 10^7$ m/s down to 10^6 m/s, depending apparently on the energy of the breakdown event and the residual conductivity of the channel. The same range of speeds is observed for dart leaders. As summarized by *Brook and Ogawa* [1977], *Ishikawa* [1961] photographed three rates of streamer progression in lightning discharges: 5×10^4 m/s, $1 - 2 \times 10^5$ m/s, and $3 - 4 \times 10^6$ m/s. Ishikawa termed these to be slow, medium, and fast streamers, respectively. *Orville and Idone* [1982] measured photographic speeds of 2.9×10^6 to 2.3×10^7 m/s for dart leaders near ground, comparable to and greater than the fast speeds of Ishikawa. Given the similarity between K type and dart streamers and the observed speed range for each, there is good agreement between the radio and optical observations. *Ogawa and Brook's* [1964] estimate of 1.3×10^6 m/s for K events is smaller than the typical values, because they underestimated the extent of the K channel and overestimated the duration of propagation. Ishikawa's medium- and slow-speed streamers may correspond to the initial-type breakdown discussed above and to the slow intracloud event of Figure 17.

As noted by *Hayenga* [1984], the K streamers immediately precede the rapid field change of the K event. Rather than the K streamer itself being a recoil event, as assumed by *Richard et al.* [1986], the K streamer would be the initiator of any recoil event (i.e., of the current increase evidenced by the rapid K field change). In this regard the K streamer would again be similar to the dart leader, which initiates the recoil-like return stroke. The interpretation of K events as a recoil phenomena originated with *Ogawa and Brook* [1964], who studied the shape of the electrostatic field change of a number of intracloud discharges and inferred that the K events, which occurred late in the flashes, were negative recoil streamers along the path of slow positive breakdown from the upper positive charge in a storm down to the level of negative charge. This inference was supported by moving-camera photographs of intracloud channels that happened to extend below cloud base, which showed that the channel brightening associated with K events propagated in the opposite direction to branching of the channel.

The composite results of Figure 4 show that the flashes branched away from the channel to ground. The K streamers and dart leaders of the flashes progressed in the direction of the channel to ground and therefore progressed in the opposite direction to the branches, in agreement with the above observations of *Ogawa and Brook* [1964]. Similar observations have been obtained by *Proctor* [1981], *Proctor et al.* [1988], and *Richard et al.* [1985]. The fact that the K streamers travel opposite to the direction of branching is a result of the retrograde manner in which the flashes develop, however, and does not in itself imply that the K streamers (or dart leaders) are recoil events. The inference by *Ogawa and Brook* [1964] that the K events were preceded by a slow downward positive streamer was obtained from single-station electric field change measurements; similar analyses of multiple station electric field measurements by *Liu and Krehbiel* [1985] and *Krehbiel* [1981] indicated the opposite, namely that intracloud breakdown starts with upward negative breakdown. The latter is also supported by the results for the initial breakdown of flash 153844 of this study (Figure 6).

Mazur [1989] has proposed that the negative K streamers are recoil events which travel backward along the channels of RF-invisible positive streamers that are part of bidirectional breakdown of previous activity. These inferences were based on indications of bidirectional breakdown in aircraft-triggered lightning and on observations by *Richard et al.* [1985] in which gaps in the channels of extensive intracloud discharges were subsequently traversed by high-speed negative streamers. K event D of Figure 8 is an example in which a fast streamer bridged a gap; component D2 of this event began at a distance from previously detected activity and propagated at a high speed (10^7 m/s) into the path of the previous activity. The event was delayed by 19 ms from the previous C activity, however, and required two attempts to get started. This, and the fact that positive streamers are observed which radiate at RF, makes it unclear that an RF-invisible phenomenon needs to be invoked or is the cause of K streamers. Rather, K streamers (and dart leaders) would appear simply to be the result of the onset of breakdown at a distance in locally enhanced fields. (Recent analyses of additional flashes observed with an improved system indicate that K streamers usually begin close to or on previously de-

tected channels and do not usually bridge gaps, which would further obviate the need for invisible streamers [*Shao*, 1993].)

Hayenga [1979, 1984] noted the similarity between the fast burst streamers of K events and what he termed "precursor" radiation associated with dart leaders of subsequent strokes to ground. Inexplicably, Hayenga's results did not show that the dart leader radiation progressed to ground. This led him to use the term "precursor" for the dart leader RF activity and to conclude that the optical and radio dart leader phenomena, although related, were not correlated. This finding was supported by the early observations of *Brook and Kitagawa* [1964] that UHF radiation during dart leaders often ceased 50 to 150 μs before the return stroke onset. The latter led Kitagawa and Brook to suggest that dart leader radiation was produced primarily within the cloud rather than by the descending part of the leader to ground.

Richard et al. [1986] found that the dart leader radiation propagated in a highly organized manner to ground at estimated speeds between 10^7 and 5×10^7 m/s. They noted that the speed values were at the high end of the photographically measured speeds of *Orville and Idone* [1982]. *Rhodes* [1989] confirmed this behavior of the dart leader radiation and obtained speed estimates that were in better agreement with Orville and Idone's measurements. Rhodes' results are documented in this paper, along with more recent results of a similar nature. In addition to progressing down the channel like the optical dart leader, the RF radiation is found to continue up to the time of the return stroke and to extinguish at the onset of the return stroke. Although we do not have correlated optical observations, there can be little doubt that the RF radiation is well correlated with the optical leader descent. Further study is required to explain *Brook and Kitagawa's* [1964] observations.

While the dart leader observations of *Richard et al.* [1986] were consistent with the idea of a descending leader, they interpreted other results of their study to be inconsistent with the generally accepted view that the channel to ground is established by the initial leader. In particular, they observed fast streamers that appeared to establish the channel to ground well before the onset of the initial leader and also at the beginning of the initial leader (events *a* and *b* of their Figure 8). Streamer *a* occurred several hundred milliseconds before the initial stroke, and streamer *b* occurred at the beginning of the apparent initial leader, 50 ms before the return stroke. Also, later streamers prior to the stroke (*c* and *d*) appeared to extend the leader channel upward rather than downward. Finally, electric field change measurements of the streamers did not agree with the assumed streamer orientation or usual leader phenomenology. From this they concluded that the radio phenomenology of breakdown prior to and during the initial leader of a discharge was uncorrelated with the electrostatic and optical phenomena.

The results of this study indicate that radiation from initial leaders, although noisier and more complex than dart leaders, progresses in an orderly manner to ground (see also *Rhodes and Krehbiel* [1989]). Breakdown during intracloud activity preceding the initial leader is confined within the cloud, and fast streamers during the initial leader propagate into rather than away from the leader channel. *Krehbiel* [1981] has shown that the electrostatic field change of initial leaders is fully consistent with a gradual and steady lowering of negative charge during the leader descent. Also, *Proctor* [1981] and *Proctor et al.* [1988] reported excellent agreement between the measured electrostatic field changes of leaders and computed field changes based on the progression of the RF source locations.

We note that the discrepancies identified by Richard *et al.* [1986] and described above can be explained if streamers *a–d* of their Figure 8 and the intracloud streamer of their Figure 11 propagated horizontally away from (or toward) their interferometer rather than vertically toward (or away from) ground. In both situations the elevation angle would decrease (or increase) with time, as if the channel were directed toward ground. This type of ambiguity is always present in single-station interferometer observations but can usually be resolved by careful examination of the overall results. Also, the streamers may have appeared to contact ground as a result of incorrect resolution of their fringe ambiguities.

Several types of radiating events have been observed during and after return strokes. For initial strokes the leader radiation is observed to continue through the onset of the return stroke and usually to increase in amplitude relative to the leader radiation. The continued radiation originates along the lower extent of the leader channel, presumably from radial breakdown into the return stroke channel. The radiation sources are observed to progress rapidly up the channel, either as one well-defined event or (in more complex situations) as a sequence of several upward propagating events (Figure 10), and also to travel out along unsuccessful branches. Radiation later during the return stroke originates in or beyond the source region of the leader. Similar results have been reported by *Proctor* [1981], *Proctor et al.*, [1988], and *Richard et al.* [1986]. *Hayenga* [1984] was unable to detect upward source motion during initial or subsequent return strokes.

For strokes initiated by dart leaders, the leader radiation usually extinguishes at the onset of the return stroke. In agreement with the results of a number of investigators, the return stroke tends to be quiet at radio frequencies [*Malan*, 1958; *Brook and Kitagawa*, 1964; *Rustan et al.*, 1980; *Proctor*, 1981; *Hayenga*, 1984; *Richard et al.*, 1986; *Proctor et al.*, 1988]. This indicates that RF radiation is associated primarily with breakdown and not with current flow such as occurs during the return stroke. Intermittent radiation is sometimes observed at locations back up along the leader channel, apparently as the upward propagating return stroke encounters branch points on the channel (Figures 13c and 13d, and 14c). This agrees with the interpretation of *LeVine and Krider* [1977]. Radiation occurs intermit-

tently along channel segments that have been recently conducting, as in the case of the leader of Figure 14c.

The quiet period of the return stroke is usually terminated by one or more bursts of radiation from the source region of the leader. Some of these bursts occur within 100–200 μs of contact with the ground and appear to be associated with the arrival of the return stroke back in the leader source region, in agreement with the inference by *Brook and Kitagawa* [1964]. Such bursts are either localized just beyond the leader source region, as in event *b* of Figure 16c, or propagate away from the source region, as in Figures 11c and 12c. The latter are positive streamers that travel at speeds comparable to the fast negative streamers of dart leaders and K events. They often are not preceded by other detectable activity and appear to establish new channel segments which are followed by the subsequent activity of the flash.

Post return stroke bursts which occur after a longer time delay, up to 1–2 ms, propagate into the leader channel as negative streamers (Figure 11d) and appear to renew the current flow along the entire channel to ground. M events during continuing currents (Figure 11d and 13c) behave in the same manner, and the two are probably the same phenomenon. *Hayenga* [1984] found downward moving sources during the post return stroke period, which presumably were also the same phenomena.

Some strokes initiated by dart leaders do not have a quiet period during the return stroke. In these instances, also noted by *Takagi* [1969] and *Hayenga* [1984], the radiation continues with decreased amplitude after the leader contacts ground (Figure 16a). The continuing radiation originates in a region that is distinctly separate from the leader source region, and is produced by breakdown which appears to have been concurrent with that of the leader, but whose presence is not revealed until the stronger radiation of the descending leader is extinguished. The concurrent breakdown appeared to establish new branches which were followed by subsequent strokes of the flash. In the example shown (Figure 16c), delayed radiation was also produced immediately adjacent to the leader start point, which appeared to be associated with the arrival of the return stroke at the top of the leader channel. This indicates that the concurrent breakdown did not produce a conducting extension of the leader channel.

The above results suggest that new branches during cloud-to-ground flashes are produced at the time of a leader-return stroke sequence, either by the action of positive streamers which are launched when the return stroke reaches the upper end of the leader channel or by breakdown which is concurrent with the leader near the leader source region. Not all strokes produce such activity, however, so that other branching mechanisms would also appear to occur.

On the basis of their results, *Proctor et al.* [1988] proposed a model of a ground flash in which breakdown immediately following a return stroke overshoots previously active regions and extends the channels primarily in vertical directions, both upward and downward from the main, horizontal channel inside the cloud. The vertical channels were found to be active during the ensuing interstroke interval, and the flashes were observed to develop in a retrograde manner horizontally through the storm, with each stroke producing a series of the vertically oriented streamers. The resulting structure of the flash was therefore envisioned to have a "herringbone" pattern. The results of the present study are consistent with horizontal development of the discharges, as found both by *Krehbiel et al.* [1979] and *Proctor et al.*, [1988]. They indicate that the flashes developed in a retrograde manner but show no evidence of a herringbone structure. Rather, the retrograde development appeared to be the result of primarily horizontal breakdown, mostly during the interstroke interval and sometimes also immediately following the return stroke. The interstroke activity consisted of negative streamers that progressed into the previous stroke channel from adjacent locations, thus extending the flash horizontally. The immediate post stroke activity consisted of positive streamers that progressed away from the stroke channel, apparently as the return stroke reached the source region of the leader (Figures 11c and 12c). This behavior has been confirmed by the analysis of a number of additional ground flashes and presents a more self-consistent picture of retrograde development than Proctor et al.'s model.

Finally, it is clear from the results of this and other studies that VHF radiation is produced by breakdown processes and not by current flow along already conducting channels. The mechanism or mechanisms by which this radiation is produced is not well understood and remains an unanswered question.

Acknowledgments. This research was supported by the National Science Foundation under grants ATM-8518165 and ATM-8117665 and by the U.S. Office of Naval Research under grant N00014-84-K-0069.

References

Brook, M., and N. Kitagawa, Radiation from lightning discharges in the frequency range 400 to 1000 Mc/s, *J. Geophys. Res., 69*, 2431-2434, 1964.

Brook, M., and T. Ogawa, The cloud discharge, in *Lightning*, vol. 1, edited by R. H. Golde, pp. 191-230, Academic, San Diego, Calif., 1977.

Hayenga, C. O., Positions and movement of VHF lightning sources determined with microsecond resolution by interferometry, Ph.D. thesis, Univ. of Colo., Boulder, 1979.

Hayenga, C. O., Characteristics of lightning VHF radiation near the time of return strokes, *J. Geophys. Res., 89*, 1403-1410, 1984.

Hayenga, C. O., and J. W. Warwick, Two-dimensional interferometeric positions of VHF lightning sources, *J. Geophys. Res., 86*, 7451-7462, 1981.

Ishikawa, H., Nature of lightning discharges as origins of atmospherics, *Proc. Res. Inst. Atmos. Nagoya Univ., 8A*, 1-274, 1961.

Krehbiel, P., An analysis of the electric field change produced by lightning, Ph.D. dissertation, Univ. of Manch-

ester Instit. of Sci. and Tech., Manchester, England, 1981.

Krehbiel, P. R., M. Brook, and R. A. McCrory, An analysis of the charge structure of lightning discharge to ground, *J. Geophys. Res., 84*, 2432-2456, 1979.

Lennon, C. L., LDAR–A new lightning detection and ranging system (abstract), *EoS Trans. AGU, 56*(12), 991, 1975.

LeVine, D. M., and E. P. Krider, The temporal structure of HF and VHF radiations during Florida lightning return strokes, *Geophys. Res. Lett., 4*, 13-16, 1977.

Liu, X.S., and P. R. Krehbiel, The initial streamer of intracloud flashes, *J. Geophys. Res. 90*, 6211-6218, 1985.

Malan, D. J., Radiation from lightning discharges and its relation to the discharge process, in *Recent Advances in Atmospheric Electricity*, pp. 557-563, Pergamon, New York, 1958.

Malan, D. J., 176 pp, *Physics of Lightning*, English University Press, London, 1963.

Mazur, V., Triggered lightning strikes to aircraft and natural intracloud discharges, *J. Geophys. Res., 94*, 3311-3325, 1989.

Ogawa, T., and M. Brook, The mechanism of the intracloud lightning discharge, *J. Geophys. Res., 69*, 5141-5150, 1964.

Orville, R. E., and V. I. Idone, Lightning leader characteristics in the Thunderstorm Research International Program (TRIP), *J. Geophys. Res., 87*, 11,177-11,192, 1982.

Proctor, D. E., A radio study of lightning, Ph.D. thesis, 574 pp., Univ. of Witwatersrand, Johannesburg, South Africa, 1976.

Proctor, D. E., VHF radio pictures of cloud flashes, *J. Geophys. Res., 86*, 4041-4071, 1981.

Proctor, D. E., R. Uytenbogaardt, and B. M. Meredith, VHF radio pictures of lightning flashes to ground, *J. Geophys. Res., 93*, 12,683-12,727, 1988.

Rhodes, C. T., Interferometric observations of VHF radiation from lightning, Ph.D. thesis, N. M. Instit. of Mining and Technol., Socorro, N.M., 1989.

Rhodes, C. T., and P. R. Krehbiel, Interferometric observations of a single stroke cloud-to-ground flash, *Geophys. Res. Lett., 16*, 1169-1172, 1989.

Rhodes, C. T., X. M. Shao, P. R. Krehbiel, R. J. Thomas, Observations of lightning processes using VHF radio interferometry, International Aerospace Conf. on Lightning and Static Electricity, NASA Conf. Publ. 3106, 68A1-68A13, Cocoa Beach, Fl., 1991.

Richard, P., and G. Auffray, VHF-UHF interferometric measurement applications of lightning discharge mapping, *Radio Sci., 20*, 171-192, 1985.

Richard, P., J. Appel, and F. Broutet, A three-dimensional interferometric imaging system for the spatial characterization of lightning discharges, paper presented at 10th International Aerospace and Ground Conference on Lightning and Static Electricity, Paris, France, 1985.

Richard, P., A. Delannoy, G. Labaune and P. Laroche, Results of spatial and temporal characterization of the VHF-UHF radiation of lightning, *J. Geophys. Res., 91*, 1248-1260, 1986.

Rustan, P. L., M. A. Uman, D. G. Childers, W. H. Beasley, and C. L. Lennon, Lightning source locations from VHF radiation data for a flash at Kennedy Space Center, *J. Geophys. Res., 85*, 4893-4903, 1980.

Shao, X. M., The development and structure of lightning discharges observed by VHF radio interferometer, Ph.D. dissertation, N. M. Inst. of Mining and Technol., Socorro, N. M., 1993.

Takagi, M., VHF radiation from ground discharges, *Proc. Res. Inst. Atmos. Nagoya Univ., 16*, 163-168, 1969.

Taylor, W. L., A VHF technique for space-time mapping of lightning discharge processes, *J. Geophys. Res., 83*, 3575-3583, 1978.

Uman, M. A., et al., An unusual lightning flash at the NASA Kennedy Space Center, *Science, 201*, 9-16, 1978.

Uman, M. A., *The Lightning Discharge*, Academic, San Diego, Calif., 1987.

Warwick, J. W., C. O. Hayenga, and J. W. Brosnahan, Interferometric directions of lightning sources at 34 MHz, *J. Geophys. Res., 84*, 2457-2468, 1979.

C. O. Hayenga, 4855 Kings Ridge Blvd., Boulder, CO 80301. (e-mail: Internet 71674.1403@compuserve.com)

P. R. Krehbiel, X. M. Shao, and R. J. Thomas, Geophysical Research Center, New Mexico Institute of Mining and Technology, Socorro, NM 87801. (e-mail: Internet krehbiel@opus.nmt.edu; xuan-min@opus.nmt.edu; thomas@crane.nmt.edu)

C. T. Rhodes, Los Alamos National Laboratories, MS D466, Los Alamos, NM 87545. (e-mail: Internet ctr@lanl.gov)

(Received December 30, 1992; revised January 10, 1994; accepted January 28, 1994.)